Characterization of the small intestinal lesion in celiac disease by label-free quantitative mass spectrometry[1]

Astrid E. V. Tutturen[*,†], Siri Dørum[*], Trevor Clancy[‡], Henrik M. Reims[§], Asbjørn Christophersen[¶], Knut E. A. Lundin[¶,‖], Ludvig M. Sollid[*,¶], Gustavo A. de Souza[†,**], Jorunn Stamnaes[*]

* Centre for Immune Regulation and Department of Immunology, University of Oslo and Oslo University Hospital-Rikshospitalet, 0372 Oslo, Norway

† Proteomics Core Facility, Oslo University Hospital-Rikshospitalet, 0372 Oslo, Norway

‡Department of Immunology, Institute for Cancer Research, Oslo University Hospital-Radiumhospitalet, 0310 Oslo, Norway;

§ Department of Pathology, Oslo University Hospital, Norway

¶ KG Jebsen Coeliac Disease Research Centre, University of Oslo, 0372 Oslo, Norway

‖ Department of Gastroenterology, Oslo University Hospital-Rikshospitalet, 0378 Oslo, Norway

** The Brain Institute, Universidade Federal do Rio Grande do Norte, 59078-400 Natal-RN, Brazil

Address correspondence to: Jorunn Stamnaes

Address: Institute of Immunology, Oslo University Hospital Rikshospitalet, Sognsvannsveien 20, 0372 Oslo, Norway. Phone: 004723074248. E.mail: jorunn.stamnas@medisin.uio.no

Number of text pages: 39

Number of tables: 2

Number of supplemental tables: 9

Number of figures: 7

Number of supplemental figures: 3

Disclosures: None declared

Running title: Global proteomics of celiac mucosa

Funding: This work was supported by grants supported by grants from the South-Eastern Norway Regional Health Authority; the Research Council of Norway through its Centre of Excellence funding scheme (project number 179573/V40). The Proteomics Core Facility is supported by a Core Facility fund from the Norwegian Southeastern Health Organization.

[1] Current addresses:
Astrid E.V.Tutturen: Department of Molecular Cell Biology, Institute for Cancer Research, Oslo University Hospital, The Norwegian Radium Hospital, Oslo, Norway
Siri Dørum: Norwegian Doping Control Laboratory, Oslo University Hospital, Oslo, Norway

ABSTRACT

Global characterization of tissue proteomes from small amounts of biopsy material has become feasible due to advances in mass spectrometry and bioinformatics tools. In celiac disease (CD), dietary gluten induces an immune response which is accompanied by pronounced remodeling of the small intestine. Removal of gluten from the diet abrogates the immune response and the tissue architecture normalizes. In this study we have quantified differences in global protein expression of small intestinal biopsies from CD patients by analyzing formalin fixed paraffin embedded (FFPE) material using liquid-chromatography mass spectrometry and label-free protein quantitation. We have compared protein expression in biopsies collected from the same patients before and after one year treatment with gluten free diet (n=10) or before and after 3-day gluten provocation (n=4). We show that differential expression of proteins in particular from mature enterocytes, neutrophils and plasma cells can distinguish untreated from treated CD mucosa, and that immunoglobulin variable region IGHV5-51 expression may serve as a CD specific marker of ongoing immune activation. In patients that had undergone gluten challenge we observed coordinated upregulation of wound response proteins including the CD autoantigen transglutaminase 2. Our study provides a global and unbiased assessment of antigen-driven changes in protein expression in the celiac intestinal mucosa.

INTRODUCTION

Global transcriptome and proteome quantification of diseased versus healthy tissue are attractive strategies to gain insight into disease mechanisms and discovery of biomarkers. Next-generation sequencing technology has boosted the field of transcriptome analysis. However, the correlation between mRNA transcript levels and protein expression levels is relatively poor. [1, 2] Thus, the importance of reliable characterization and quantification of cell and tissue proteomes are increasingly appreciated. Global, label free protein quantification by use of mass spectrometry has in the recent years emerged as a sensitive tool for detection of differential protein expression. [3] Also formalin fixed paraffin embedded (FFPE) tissue collected for routine pathology analysis can successfully be used for mass spectrometry analysis and identification and quantification of several thousand proteins. [4-6]

Celiac disease (CD) is a prevalent intestinal disorder that occurs in genetically susceptible individuals. The disease is driven by a CD4+ T-cell response towards dietary gluten proteins. [7] This results in inflammation in the small intestine accompanied by tissue remodeling, villous blunting and loss of intestinal surface area. The intestinal lesion is infiltrated with immune cells, in particular intraepithelial lymphocytes and IgA+ plasma cells. [8-10] On average 10% of the plasma cells produce autoantibodies towards transglutaminase 2 (TG2), an endogenous enzyme that catalyzes post-translational modification of gluten T-cell epitopes. [11-13] HLA-DQ-restricted CD4+ T-cells that recognize these gluten epitopes exhibit a pro-inflammatory phenotype and secrete high amounts of IFN-γ. [14-16] CD patients also have increased numbers of CD8+ intraepithelial T cells that contribute to tissue destruction and intestinal remodeling as these cells, by use of NK-cell receptors, kill stressed enterocytes. [17]

Disease severity in CD can be graded according to the degree of histological changes in the intestine, and is often sub-classified to six groups, ranging from Marsh 0 (M0) to Marsh 3C (M3C). [18] M0 describes the normal histology. M1 describes the same overall villous structure with long villi, short crypts but more than 25 intraepithelial lymphocytes per 100 enterocytes. M2 has the same features but with crypt hyperplasia. M3A-C describes the range from partial to sub-total to total villous atrophy. Many of these morphological changes are reversible, and removal of gluten from the diet often leads to recovery and normalization of the small intestinal architecture. [19]

The disease specific adaptive immune response in CD is well characterized. This may be one of the reasons why few "omics" studies have been conducted on celiac intestinal tissue. [20-22] However, many questions still remain unanswered, and *a priori* knowledge on disease mechanisms should encourage bottom up transcriptome or proteome expression studies. Such efforts will generate data that can both support and supplement, or challenge, established knowledge. In this study we have performed an in-depth analysis of the small intestinal celiac mucosa applying a quantitative liquid chromatography tandem mass spectrometric (LC-MS/MS) proteomics approach, where we have analyzed tissue from FFPE blocks collected for routine histology assessment. We have compared protein expression levels in biopsies collected from the same patients before or after dietary intervention: First we compared protein expression in biopsies collected from ten patients with untreated CD (UCD) with biopsies collected one year later after treatment with gluten free diet (GFD) (treated CD; TCD). We next analyzed tissue from four TCD patients that developed morphological changes on day 4 in response to 3-day gluten challenge. Our data showed differential expression of proteins that agree with our current understanding of CD pathogenesis and but also suggests that changes in protein expression may not always correlate with histology. We

identify immunoglobulin (Ig) gene family usage which may serve as a disease specific marker of immune activation. Patients subjected to 3-day gluten challenge displayed coordinated regulation of proteins indicative of acute wound response and tissue remodeling. This provides insight into the initial steps of intestinal remodeling in response to gluten in CD.

MATERIALS AND METHODS

Patient selection and patient material

Fourteen DQ2.5+ CD patients were selected for *post-hoc* analysis from two patient cohorts previously enrolled in research projects in our lab: In the first group we compared biopsies collected from 10 CD patients at the time of diagnosis (UCD) with biopsies collected one year later following treatment with GFD (TCD) (Christophersen *et.al*; manuscript in preparation). All patients were classified as M3 at the time of diagnosis and the majority recovered to M0-1 one year later (Patient P1-P10; Table 1). The second group of patients consisted of 4 TCD patients that developed histological changes in response to a three-day gluten challenge. [23] We analyzed biopsy material collected on day 0 before challenge and biopsies collected on day 4 after challenge (Patient B-E; Table 2). Material from duodenal biopsy blocks collected for histology assessment was utilized in this study. For patients P1-P10 we report anti-TG2 IgA levels and intraepithelial lymphocytes (IEL) numbers (per 100 enterocyte) assessed at the time of diagnosis and after one year follow up (Table 1) (Christophersen *et.al*; manuscript in preparation). All patients had given informed and written consent and the use of material was approved by Regional Committee for Medical and Health Research Ethics (REK 2010/2720).

147 **Preparation of FFPE tissue section digests**

148 Fifteen 5-micrometer-thick sections were cut from each FFPE biopsy block and collected in a
149 tube (1.5 ml, Eppendorf, Hamburg, Germany). Paraffin was removed by the following
150 procedure. Paraffin Removal Reagent (1 ml, BiOstick, MO BIO Laboratories, Qiagen,
151 Carlsbad, CA, USA) was added and incubated for three minutes at 55 °C with gentle agitation
152 (350 rpm). The samples were centrifuged at 14000 x g for five minutes and the supernatant
153 was removed. Xylene (1 ml, AnalR Normapur, VWR Chemicals, Radnor, PA, USA) was
154 added and the previous step was repeated. Ethanol (absolute, 1 ml, AnalR Normapur, VWR
155 Chemicals) was added and incubated for 5 minutes at room temperature with gentle agitation
156 (350 rpm), before centrifugation as above and removal of supernatant. The purification step
157 with ethanol was repeated, but incubation time was 1 minutes. Traces of ethanol were
158 removed from the samples by incubation in a vacuum drier. For protein extraction the sample
159 tissues were dissolved in 20 µl 0.2 % ProteaseMax Surfactant (trypsin enhancer, Promega,
160 Madison, WI, USA) in 50 mM NH_4HCO_3 and 73.5 µl 50 mM NH_4HCO_3 were added. The
161 samples were sonicated in water bath for 60 minutes and further incubated at 98 °C for 90
162 minutes on a heating block. The samples were quickly spun down every 10^{th} minutes to avoid
163 liquid accumulation in the lid. The samples were slowly cooled down to room temperature
164 and frozen at -20 °C overnight. The samples were thawed and sonicated in a water bath for 60
165 minutes. Protein concentration was measured using DirectDetect (Millipore, Merck,
166 Darmstadt, Germany). For trypsin digestion, the whole extracts were used (protein
167 concentrations ranged from 20 to 37.4 µg) and lysozyme (from chicken, egg white, BioUltra
168 lypholyzed powder, >98%, >40.000 units/mg protein) was spiked-in to a final concentration
169 of 0.2 % (w/w). For enzymatic digestion 1 µl 1 % ProteaseMax Surfactant and 0.5 µg trypsin
170 was added and incubated at 37 °C in a wet chamber overnight. ProteaseMax Surfactant was
171 degraded by adding trifluoroacetic acid to a final concentration of 0.5 % and the samples were

vortexed and incubated for five minutes at room temperature before centrifuged for 10 minutes at 14 000 x g.

LC-MS/MS analysis

Prior to LC-MS/MS analysis the samples were desalted by reversed phase chromatography using C18 micro columns prepared by stacking three layers of C18 Empore Extraction Disk (Varian, St. Paul, MN, USA) into 200 µl pipet tips. For samples from patients P1-P10 (Table 1), reference peptides (150 fmol, MassPREP Digestion Standard Mix 1, Waters, Milford, MA, USA) were spiked-into each sample, before samples volume was adjusted to 14 µl using 0.1 % formic acid. Samples were analyzed in three technical replicates on a Q Exactive hybrid quadropole-orbitrap plus (Thermo Scientific, Thermo Fisher Scientific, Waltham, MA, USA) interfaced with an EASY-nLC 1000 (Thermo Scientific). Peptides were separated on a 50 cm EASY Spary PepMap®RSLC column (C18, 2 µm, 100Å, 75 µm inner diameter, Thermo Scientific) using a 300 minutes gradient; 2-19% B in 19 minutes, 19-22%B in 156 minutes and 22-35%B in 125 minutes (solution A: water with 0.1% formic acid, solution B: acetonitrile with 0.1 % formic acid). The mass spectrometer was operated in a data-dependent mode, top 10 MS/MS scans using a MS scan range of 400-1200 *m/z*. Following parameters for MS scan were applied: resolution: 70.000 at m/z 200, AGC target: 3e6 and maximum IT: 100ms. The MS/MS scan were performed at: resolution: 17.500, AGC target: 1e5, maximum IT: 100ms, isolation window: 2.0 *m/z*, NCE: 25, under fill ratio: 1.0%, intensity threshold: 1.0e4 and dynamic exclusion: 30.0s. Samples from patient B-E (Table 2) were analyzed by similar conditions as described above behalf from that the instrument was an Q Exactive hybrid quadropole-orbitrap (Thermo Scientific) and peptide separation was performed on a 25 cm EASY Spray PepMap®RSLC column (C18, 2 µm, 100Å, 75 µm inner diameter, Thermo

Scientific) using a 300 minutes gradient; 2-30% B in 300 minutes. Isolation window was set to 3.0 m/z for MS/MS scans.

Database search

Protein identification and label-free quantitation was performed using the MaxQuant software package (version 1.5.1.2). [24] MS and MS/MS spectra were searched by the Andromeda search engine [25] against the UniProtKB FASTA database for the human proteome (85,915 entries including isoforms and canonical sequences, downloaded from www.UniProt.org, October 2014) in addition to a FASTA database of spiked in proteins for patients P1-P10. The following parameters were applied: enzyme: Trypsin with no proline restriction; variable modifications: deamidation (NQ), oxidation (M), acetylation (protein N-term), Gln-pyro (Q), and pyro-Glu (E). The first search was performed with mass tolerance of 20 ppm for precursor ion and after recalibration a 6 ppm tolerance was used in the main search; mass tolerance for fragment ions was set to 20 ppm. Minimal unique peptides were set to 1 and a false discovery rate of 0.01 was used in all instances. For identification, "match between runs" was enabled, and quantification was done using the MaxQuant label free quantification algorithm with a minimum ratio count of one. Data from patient P1-P10 (Table 1) and patient B-E (Table 2) were analyzed separately. For Ig gene identifications, data from P1-P10 were searched against a FASTA database generated from amino acid sequences of human Ig families obtained from the International ImMunoGeneTics Information System (IMGT) database, [26, 27] and the FASTA database for spike-in proteins using the same parameters as above. All data are fully available at ProteomeXchange repository [database *Note to referees: data will be uploaded to the Proteome Xchange repository*]

Statistical analysis

Perseus software (version 1.5.0.31) was used to perform statistical analysis of LFQ intensities. Proteins considered by MaxQuant to be possible contaminants, hits from reverse sequences (FDRs) or "only identified by site" were removed from the list of identifications for all datasets prior to statistical analysis. Protein groups identified by one peptide and quantified by one LFQ ratio were not excluded from downstream analysis. Proteins highlighted in the results and discussion were quantified by LFQ >1. Biopsies were grouped in two categories: TCD or UCD for P1-P10, or "before" and "after" for patients B-E. An imputation approach was used to replace the zero values by randomly generated values selected accordingly to the normal distribution of the data in order to simulate the distribution of low abundant proteins. [28] Principal component analysis was done on log 2 transformed LFQ intensities following imputation of zero values. T-test was performed using a p-value of <0.01 as threshold for P1-P10 and p-value of <0.05 for patient B-E; S0= 0.5 and further FDR correction using a permutation-based method allowing 250 randomizations for both groups. Volcano plots were created using the same parameters. Sample hierarchical clustering was done in Perseus on t-test significant proteins using log2 transformed LFQ values, where zero values were replaced by imputation as described above, choosing Euclidian distance for row tree generation and Speerman correlation for column tree generation. Colors indicate log2 LFQ intensity. Protein intensity graphs show median values of log2 LFQ intensities following imputation of zero values. For Ig gene identifications, contaminants were filtered out as above and only proteins with valid values in at least 50% of TCD or UCD groups were included. Imputation of zero values was done based on total matrix expression following log2 transformation. Protein identifications from the spike-in database and two Ig protein groups assigned to open reading frames were removed prior to statistical analysis. Median values for sample triplicates were

used for principal component analysis and t-test comparison visualized as volcano plot (two-sample t-test, $p<0.05$ S= 0.5).

Bioinformatic analysis

Cytoscape [29] version 3.3.0 was used with the plug-in ClueGO [30] to address enrichment of Gene Ontology (GO) biological processes. The gene list corresponding to proteins with reduced or increased expression (t-test significant, from Perseus) was used. If more than one gene name was given for the identified protein group, the first gene name was selected. Some protein identifications that were not assigned to unique genes (e.g. immunoglobulin entries) were not included in enrichment analysis. Default settings were used. GO Term fusion was chosen and only pathways enriched by $p < 0.05$ were shown. Grouping was based on kappa score with initial group size of 1 and 50% genes or terms for group merge. Networks were visualized in CytoScape and further color coded using Adobe Illustrator (CS5.1). Proteins upregulated in P1-P10 were also searched for GO Reactome pathway enrichment.

Protein-protein interaction network analysis

For patient P1-P10 (UCD vs TCD), a custom protein-protein interaction (PPI) network was built by selecting seed genes that were t-test significant from Perseus (p-value <0.01) and allowing those seed genes to generate PPI networks from an integrated database of protein interactions [31]. Each PPI in the network had at least one PubMed citation, was experimentally validated, and was a physical binding interaction. Only protein interaction neighbors detected in the proteomics dataset were allowed to form interactions in the PPI network generation. A filter was applied whereby only proteins annotated to the GO term “response to cytokine” (GO:0034097) were allowed to be included in the PPI network. The network was then

visualized and annotated using the Cytoscape version 3.3.0 and all proteins were labelled as increased or decreased in UCD vs TCD based on the fold change in expression as calculated from the t-test analysis in Perseus. Proteins present in the GO terms "response to type I interferon" (GO: 0034340), "response to interferon gamma" (GO: 0034341) or "response to tumor necrosis factor" (GO: 0034612) were color coded as indicated.

For patient B-E (before and after 3-day challenge) PPI analysis was performed using STRING. [32] T-test significant upregulated proteins (84, $p<0.05$) from Perseus were analyzed resulting in 83 nodes (proteins) and 135 edges (interactions). The network was exported and further color coded in Adobe Illustrator CS5.1. Nodes (proteins) with no edges (interactions) were removed from the network.

Immunoenzyme staining and estimation of cell densities

Tissue sections from FFPE biopsy blocks of 5 patients (P1, P2, P5, P6, P10; UCD and TCD) were subjected to immune-enzyme staining to enumerate CD15, MPO and calprotectin expressing cells. Three micrometer thick sections were stained using the Dako EnVisionTM Flex+ System (K8012; Dako, Glostrup, Denmark) and the Dako Autostainer. Deparaffinization and epitope retrieval was performed using PT-Link (Dako) and EnVisionTM Flex target retrieval solution. Endogeneous peroxidase was blocked using 0.3% hydrogen peroxide for 5 min. Sections were incubated for 30min at room temperature with primary antibodies (rabbit polyclonal anti-calprotectin, 1:10000 (gift from I. Dale (Calpro, Oslo, Norway)) rabbit polyclonal anti-MPO (1:1000, A0398, Dako) or mouse monoclonal IgM anti-CD15 (1:50, clone Carb-3, Dako) followed by 15 min incubation with EnVision FLES+ rabbit or mouse linker. Sections were incubated with secondary antibodies for 30 min

292 at room temperature followed by 393-diamonibenzidine tetrahydrochloride (DAB) for 10 min
293 and counterstaining using hematoxylin.

294 Stained sections were scanned (Pannoramic MIDI, 3DHistech, Budapest, Hungary), exported
295 and analyzed using the QuPath software (0.1.2) [33], blinded to patient number and diagnosis.
296 Four to 6 representative regions of lamina propria (ranging from 30000-90000 μm^2) were
297 annotated per slide, spanning from the subepithelial basement membrane to the muscularis
298 mucosae when possible. DAB positive cells were counted using the "positive cell detection
299 tool". Only cells that were considered highly positive were counted, and positive selections
300 were manually verified. Reported values represent mean values from all counted regions.
301 Representative regions of CD15 staining from two patients were exported to Image J and
302 saved as TIF.files.

303

304 **Multi-color immunofluorescence staining**

305 Three micrometer thick FFPE tissue sections of 3 patients (P6, P5 and P2) were dewaxed and
306 subjected to antigen retrieval by heat (95°C in water bath for 20 min) using Dako antigen
307 retrieval solution (Dako). Tissue sections were blocked for 30 min in 1.25% IgG-free BSA
308 (Jackson Immunoresearch, West Grove, PA, USA) at room temperature. Primary antibodies
309 were applied over night at 4°C followed by secondary antibodies for 90 min at room
310 temperature. The primary antibodies against CD15, MPO and calprotectin were the same as
311 used for immunoenzyme staining. In addition, anti-CD163 (mouse monoclonal IgG_1, 1:1000,
312 clone 10D6, Dako) was used. Secondary antibodies were donkey-anti-mouse-IgM-A488 (115-
313 545-075, Jackson ImmunoResearch), goat anti-mouse-IgG_1-Cy3 and goat-anti-rabbit-A647
314 (both Southern Biotechnology Associates). Nuclei were counterstained with 40,6-diamidino-
315 2-phenylindole (DAPI) and slides were mounted with homemade poly(vinyl alcohol). Images

were acquired with an Olympus Fluoview FV1000 laser scanning confocal microscope (Olympus, Tokyo, Japan) using an Olympus UPlanAPO 20/0.8 oil lens (Olympus) and the FV10-ASW V4.2 software (Olympus). Images were processed and assembled using FIJI/Image J. [34, 35]

RESULTS

Comparison of protein expression in UCD vs TCD mucosa

We analyzed FFPE tissue sections from biopsy blocks of 10 patients with CD by LC-MS/MS, comparing biopsies collected at the time of diagnosis (UCD) with biopsies collected one year later after treatment with GFD (TCD). Proteins were quantified using the LFQ algorithm implemented in the MaxQuant software which allows for comparison of samples analyzed in individual LC-MS runs. [24, 36] We initially verified the normalization by spiking all samples with four different predigested proteins and one intact protein as described in Materials and Methods. The spiked-in proteins showed comparable LFQ intensities for all samples, except for patient P9 after treatment (sample 18, Supplemental Figure 1). However, total protein recovery for this sample was also extremely low (data not shown) and it was therefore removed from the dataset. We identified in total 4711 proteins (Supplemental Table 1). Principal component analysis on log2 transformed LFQ intensities of all proteins separated our data according to UCD or TCD except for two UCD samples (P7 and P8) that clustered as TCD (Figure 1A). From the underlying protein distribution along Component 1 (Figure 1B) we see that proteins likely deriving from neutrophils and monocytes (e.g. LTF, MPO) and proteins likely deriving from mature enterocytes (e.g. CYP3A4, LCT) drive this clustering (Figure 1B). Thus, we can distinguish samples from UCD and TCD mucosa based on the global proteome expression level. Comparing our ten UCD samples with nine TCD samples we found differential expression of 322 proteins ranging from 1.6 to 18.2-fold difference in

expression (two-sample t-test, FDR<0.01). We found 175 proteins with higher expression in UCD and 147 proteins with higher expression in TCD (Supplemental Table 2) as visualized by a volcano plot, where selected proteins are highlighted in red (Figure 1C). Hierarchal clustering of log2 transformed LFQ intensities for these proteins showed grouping according to TCD or UCD (green and red bars) again with the exception of the P7 and P8 UCD samples (Figure 1D). These two patients differed from the other UCD M3 patients on the protein level, despite similar Marsh classification. In our paired material, one patient (P10) did not recover to M0-1 but remained M3B after treatment. This was reflected by longer distance from the remaining TCD M0-1 samples in the dendogram (Figure 1D).

Processes related to enterocyte function are enriched in TCD mucosa

To address whether our differentially expressed proteins derive from one or more upregulated biological processes, we performed Gene Ontology (GO) biological process enrichment analysis using the ClueGO application in Cytoscape. [30] Analysis of 144 unique genes from the 147 proteins with increased expression in TCD showed enrichment for multiple processes related to nutrient metabolism and enterocyte function (Figure 2A). Reduced expression of these proteins in UCD agrees with the histological appearance of M3 with villous blunting, crypt hyperplasia and reduced numbers of mature enterocytes. Proteins annotated to the enriched processes are listed in Supplemental Table 3. We compared log2 transformed LFQ intensities of selected enterocyte derived proteins for all patients except P9 and found that Villin (VIL1) which is expressed in all enterocytes, increased only modestly upon treatment (TCD). In contrast we observed a clear increase in expression for enterocyte function related proteins, including CYP3A4, CYP2C9, LCT and FABP2 (Figure 2B). Thus, the biggest difference between the groups is due to difference in enterocyte maturation status rather than total enterocyte number as assessed from VIL1. Patients P7 and P8 UCD samples showed

high expression of enterocyte derived proteins, in particular for CYP2C9, despite classification as M3B (Figure 2B, P7 and P8; red and blue squares respectively). This likely explains why these samples failed to cluster with the other UCD patients (Figure 1A and 1D). No available clinical parameters differentiated these subjects from the remaining cohort (Table 1 and data not shown). We may speculate whether these patients initiated a gluten free diet prior to the gastroduodenal endoscopy. Reduced gluten ingestion from the time of referral to the time of endoscopy might be sufficient to induce alteration in the enterocyte status and the mucosal proteome without affecting intestinal morphology. [37] Patient P10, which remained M3B after treatment, also recovered some expression of enterocyte derived proteins, albeit at lower level than patients recovering to M0-1 (Figure 2B, blue circles). This suggests increased enterocyte maturation despite incomplete histological recovery. In contrast to other enterocyte derived proteins, we found ESPR1, an epithelial specific splicing regulator, to be overall higher expressed in UCD compared to TCD. Potentially, this could be due to the increased proliferation and differentiation of enterocytes in UCD. Over all, our data supports the notion that enterocyte maturation and function as assessed on the protein level can distinguish between TCD and UCD also in cases of incomplete histological recovery.

Processes related to immune response and plasma cell function dominate in UCD mucosa

The 175 proteins with increased expression in UCD were assigned to 152 unique genes for GO biological process enrichment analysis (Supplemental Table 2). We found enrichment of several immune response processes such as defense responses, antigen processing and presentation and B-cell activation (Figure 3A). Processes related to ER stress and response to ER stress, were also enriched. These likely reflect the massive protein synthesis machinery

that operates in plasma cells, which are abundant in the celiac lesion. Proteins annotated to the enriched processes are listed in Supplemental Table 4.

Differentiation of UCD and TCD based on immunoglobulin gene family expression

A large proportion of the plasma cells in UCD produce disease specific antibodies targeting TG2 or deamidated gluten. Antibody responses to both antigens show stereotyped and biased usage of Ig variable region genes. [11, 38-40] Many proteins in our dataset derived from identification of Ig fragments. Variable region Ig sequences are incompletely covered and poorly annotated in the Uniprot database. Thus, to address whether Ig gene family usage could be assessed from our data we searched against a dedicated Ig sequence database based on IMGT sequences as described in Materials and Methods. LFQ normalization was found to be equivalent to our Uniprot derived dataset (Supplemental Figure 2). Following filtering as described in Materials and Methods, we identified 42 Ig gene family members including 34 variable region families (Supplemental Table 5). Principal component analysis of log2 transformed LFQ intensities separated UCD from TCD samples (Figure 3B and C). The vast majority of identified Ig sequences showed increased expression in UCD compared to TCD (two-sample t-test FDR<0.05, Figure 3D). In particular three Ig variable regions separated UCD from TCD based on fold change in expression (IGKV3-15D, IGKV3-11 and IGHV5-51). Of these three Ig variable regions, we found that only IGHV5-51 decreased consistently in all patients following treatment (except for patient P7) (Figure 3E).

Increased expression of proteins derived from neutrophils in UCD mucosa.

Many of proteins with the highest fold increase in UCD compared to TCD mucosa are typically produced by neutrophils (Figure 1C). ClueGo Reactome pathway enrichment

analysis showed that 26 of the proteins with increased expression in UCD mapped to the pathway "Neutrophil degranulation" (Figure 4A and Supplemental Table 6). Some of these proteins are, however, also produced by other cells such as monocytes/ macrophages. To address whether this protein signature derives from neutrophils or other cells, we counted neutrophils (CD15 positive cells) and cells expressing two of the differentially expressed proteins (MPO and calprotectin (heterodimer of S1008A/S1009A)) by immunoenzyme staining. We found that neutrophils were increased in UCD samples, but the degree of infiltration varied between patients (Figure 4B). Neutrophils were low or absent in TCD samples from all patients. The number of cells expressing MPO was comparable to the number of neutrophils, and was low in all TCD samples. In contrast, calprotectin staining was observed in many cells in UCD and positive cells decreased but did not disappear upon treatment (TCD). The differences in cell density agree well with the protein expression levels detected by mass spectrometry in these patients (Figure 4C). To better address which cells contribute to the protein signal we observe by mass spectrometry, we also performed co-staining of cells by immunofluorescence analyzing for expression of CD15 (neutrophils), CD163 (macrophages) and MPO or calprotectin (Figure 4C). Neutrophils showed strong staining both for MPO and calprotectin. We observed very few MPO positive cells that were not neutrophils. In contrast, calprotectin staining was observed also in other cells, including TCD samples where neutrophils were absent. Some of the calprotectin positive cells also stained weakly for CD163, indicating that these cells have a myeloid origin. From these data we conclude that many of the differentially expressed proteins detected by mass spectrometry primarily derive from neutrophils in UCD, but that some proteins, like calprotecin, can to some degree also derive from monocytes/ macrophages.

Response to cytokines in UCD mucosa

Gluten specific effector CD4+ T-cells are crucial for the pathogenesis of CD. These cells are low in total number in the celiac lesion but exert their actions through secretion of pro-inflammatory cytokines. [41] Cytokines themselves are rarely detected in tissue proteome studies using mass spectrometry. [42] Identification of cytokine involvement therefore relies on detection of downstream effects. Among the biological processes enriched in UCD mucosa we find both "interferon-gamma-mediated signaling pathway" and "type I interferon signaling pathway" (Figure 3A and Supplemental Table 4). For our ClueGo enrichment analysis we only considered the t-test significant proteins. To address if we could detect additional proteins involved in response to cytokines in our dataset, we performed a protein-protein interaction (PPI) analysis where all identified proteins were considered. The t-test significant proteins were used as seeds to build the network which was then filtered to only include proteins annotated the GO term "response to cytokine". All proteins were categorized as up or downregulated based on their fold change in expression, irrespective of t-test significance. From this network we see that the majority of interacting proteins in our dataset that are part of response to cytokines, are found in the GO terms "response to type I interferon" (blue nodes), "response to interferon gamma" (yellow nodes) or "response to tumor necrosis factor" (purple nodes) (Figure 5A). Most of these proteins showed higher expression in UCD mucosa (red node border) compared to TCD mucosa (green node border). Several of the most differentially expressed proteins (e.g. STAT1) are shared between these cytokine responses. However, cytokine specific responses are transmitted by generation of different protein complexes: Type I interferon signaling is mediated by the trimeric complex of STAT1, STAT2 and IRF9 whereas IFN-γ signaling is mediated by STAT1 homodimers. [43] From the LFQ intensities, we see that STAT1 and the IFN-γ induced protein GBP1 were more abundant than STAT2 and IRF9, which may suggest that response to IFN-γ dominates over response to

type I interferon (Figure 5B). TNF response proteins TRADD and RIPK1 are also less abundant than e.g. GBP1. Most patients showed reduced expression of these proteins following treatment, with the exception of patients P6 and P10 (red and blue circles respectively; Figure 5B). Whereas STAT1 and GBP1 expression decreased, both patients showed increased expression of STAT2, IRF9, TRADD and RIPK following treatment. P6 also showed aberrantly high expression of MX1, and MX1 expression increased in both patients following treatment. Thus, from our data we can infer that our UCD patients show decreased IFN-γ signaling following treatment. In addition, two of the patients displayed protein expression patterns indicative of an ongoing type-I interferon response, independent of dietary gluten.

Characterization of M3 mucosa in response to short term oral gluten challenge

The M3 lesion of CD patients at the time of diagnosis has typically developed over time. It hence represents a state of chronic inflammation that may not provide information about the initial changes that occur upon remodeling in response to dietary gluten. Upon reintroduction of gluten, TCD patients can develop morphological changes within weeks and in some cases also within a few days. [44-47] Short term (3-day) oral gluten challenge is sufficient to recruit disease specific T cells to the blood on day 6 as detected by flow cytometry, and some few patients also develop clear morphological changes in the intestine on day 4 after initiation of challenge. [48-50] This could be considered an early stage of M3 lesion that is likely to differ from the M3 lesion of UCD patients despite identical histological classification. We analyzed biopsy material from 4 TCD patients that all developed morphological changes on day 4 in response to 3-day gluten challenge (Table 2). [49] Comparing biopsies collected before (day 0) and after gluten challenge (day 4) we identified in total 4474 proteins where 187 proteins were differentially expressed (88 proteins with increased expression and 99 proteins with

decreased expression on day 4, two-sample t-test, FDR<0.05) (Figure 6A, Supplemental Table 7 and 8). Hierarchical clustering of log2 transformed LFQ intensities of the differentially expressed proteins showed that our samples indeed cluster as "before" or "after" gluten challenge (Figure 6B). Similar to UCD M3 mucosa, we observed reduced expression of enterocyte derived proteins and increased expression of neutrophil and monocyte derived proteins on day 4 after gluten challenge (Figure 6A). Both neutrophils and monocyte-derived cells have previously been shown to increase on day 4 in this patient cohort. [51] By contrast, proteins hallmarking plasma cells were not markedly increased on day 4 (data not shown).

Short term gluten challenge induces inflammation, tissue remodeling and wound healing processes.

GO biological process analysis of 85 unique genes from 88 proteins with increased expression day 4 showed enrichment for processes related to acute inflammation, tissue organization and remodeling (Figure 7A). This includes innate defense responses, muscle contraction and cell-substrate junction assembly (Supplemental Table 9). Notably, the majority of the proteins with increased expression after gluten challenge interact with each other as determined by STRING protein-protein interaction analysis, suggesting that they are co-regulated and part of a coordinated tissue response (Figure 7B). Most of these proteins showed increased expression in all four patients on day 4 irrespective of Marsh score on day 0, although the biggest change was observed for patients B and E, who progressed from M0-1 to M3A-B (Figure 7C). Also the CD autoantigen TG2 (TGM2) was upregulated in three of four patients in response to 3-day gluten challenge (Figure 7C). In contrast, these proteins did not decrease in response to treatment in patients P1-P10 (Figure 7C). Thus, global proteome analysis of biopsies collected shortly after gluten exposure captures the early phases of tissue remodeling in the celiac small intestine

DISCUSSION

This study represents the first global proteomics characterization of the celiac small intestine by use of label free quantitative mass spectrometry. We have compared changes in proteome expression following removal or reintroduction of gluten, using material from FFPE small intestinal biopsies collected for histology assessment. Our study demonstrates that such material can be used to characterize and stratify diseased tissue on the protein level. We find differential expression of proteins that corroborate known features of CD such as loss of mature enterocytes, response to cytokines and abundance of plasma cells. In several patients we also see differential expression canonical neutrophil derived proteins. We show that expression of IGHV5-51, the variable gene used by epitope 1 anti-TG2 autoantibodies, decreased in all patients in response to GFD diet. We also compared protein expression in four patients that developed morphological changes on day 4 in response to gluten challenge. Here we observed coordinated upregulation of proteins involved in tissue remodeling and wound response which shed light on processes that occur early in the intestinal recall response towards gluten.

Our data captures many of the canonical features of the immune response of the celiac lesion, in particular the abundance of plasma cells. Notwithstanding, the most differentially expressed proteins in our datasets are typically expressed by neutrophils (e.g. MPO, LTF, AZU1, S100A8, S100A9). Some of these proteins can also be expressed by monocytes/ macrophages, which are increased both in UCD and in TCD in response to gluten challenge. [52] We verified the presence of neutrophils in our UCD samples by immunohistochemistry, and demonstrated that neutrophils express high amounts of both MPO and calprotectin. Neutrophils were close to absent in TCD patients. Thus, conceivably the dramatic change in

protein expression detected by mass spectrometry reflects neutrophil infiltration. Possibly, high protein content of stored neutrophil granules could facilitate detection of these proteins so that relatively few cells are required to give a strong protein signal. Previously, gene expression studies have shown increased transcript levels of several canonical neutrophil derived proteins in CD patients, and neutrophil infiltration has been reported in celiac lesions. [21, 53, 54] Collectively, available observations advocate further investigations into the role of neutrophils in the pathogenesis of CD.

Due to their relatively low abundance, cytokines are rarely detected by mass spectrometry analysis of total tissue digests, which is in contrast to mRNA expression studies. Therefore, an assessment of cytokines is better evaluated by expression of their downstream induced proteins. A hallmark of CD is the accumulation of pro-inflammatory gluten-reactive CD4+ T cells that produce high amounts of IFN-□ in the intestinal lesion, in addition to cytokines such as IL-21 and TNF. [15, 55] These cells are likely necessary but not sufficient to cause intestinal remodeling which may also require innate cytokines such as IL-15 and type I interferons to sufficiently disrupt tissue homeostasis, and promote enterocyte killing by cytotoxic intraepithelial lymphocytes. [7] We observed increased expression of many proteins indicative of active cytokine signaling in UCD, in particular response to IFN-□ but also to type I interferon and TNF. The different expression level of these proteins suggest dominance of IFN-□ response over type I interferon, which would agree with previous studies showing lower expression levels and large patient to patient variability for type I interferon. [56, 57] Response to IL-15 was not detected by our approach. Notably, patients P6 and P10 displayed protein expression patterns indicative of an ongoing type-I interferon response independently of dietary gluten, and P6 showed unusually high expression of MX1 both at the time of diagnosis and following treatment.

Identification of non-invasive markers to monitor intestinal recovery and diet adherence in CD is important as it can eliminate the need for biopsy evaluation in the follow-up of patients after diagnosis. Proteins we found to have higher expression in TCD vs UCD mucosa can potentially serve as such markers. Most of these proteins derive from enterocytes. The highest fold change in expression was observed for the enzymes CYP3A4, CYP2C9 and LCT, followed by proteins involved in cellular metabolism and enterocyte structure (e.g. SCIN and ESPN which are important for microvilli formation). Enzymes are good biomarker candidates as assessment of their activity can serve as a measure of enterocyte vitality. This has already been explored in human subjects for CYP3A4 by monitoring oral bioavailability of simvastatin which is predominantly metabolized by intestinal CYP3A4.[58, 59] Indeed, simvastatin was found to have high oral bioavailability in UCD patients reflecting lower CYP3A4 activity.[59] From our data also CYP2C9 emerge as a candidate marker. Both CYP2C9 and LCT can distinguish between the majority of UCD samples and patients P7 and P8 which we found to differ from the remaining UCD patients. Analysis of expression of these enzymes can possibly be superior to CYP3A4-monitoring for stratification of UCD patients, but their expression pattern must first be verified in larger patient cohorts. Enterocyte damage can also be monitored by measuring FABP2 protein in serum and urine. [60] Both retrospective and prospective studies have shown correlation between serum FABP2 levels, Marsh score and response to gluten free diet in CD patients.[61] [37, 62] We observed decreased expression of FABP2 in UCD mucosa which agrees with damage and loss of enterocytes and release of this protein into serum.

Proteins that are overexpressed in UCD may also serve a biomarkers based on their reduced expression in response to treatment. Most of the proteins we found to have higher expression

590 in UCD derive from immune response processes where a change in protein expression can be
591 induced by stimuli other than dietary gluten. In contrast, the autoantibody-response towards
592 TG2 is gluten dependent and highly disease-specific. We identified a number of different Ig
593 sequences from our FFPE material. Of these, IGHV5-51 decreased unanimously following
594 one year of treatment (except for patient P7). IGHV5-51 is the canonical heavy chain variable
595 region used by epitope 1 anti-TG2 antibodies, which are found in all untreated CD patients. [11,
596 39, 40] We propose that IGHV5-51 expression could represent a disease specific measure of
597 intestinal immune activation in CD.
598
599 Three of our 10 patients that were analyzed before and after GFD showed protein expression
600 patterns that did not correlate with their Marsh classification. Two patients (P7 and P8) were
601 classified as M3B at the time of diagnosis (UCD) but were more similar to TCD patients on
602 the protein level. One patient (P10) showed increased expression of several enterocyte derived
603 proteins such as CYP3A4 following treatment, despite classification as M3B. Discrepancy
604 between protein expression and histology has previously been noted. In agreement with our
605 observations for P10, CYP3A4 function was reported to increase following treatment despite
606 incomplete normalization of histology. [59] This argues that histology alone may be insufficient
607 to assess enterocyte vitality in CD. Our global proteomics analysis supports the assessment of
608 enterocyte vitality as measure for intestinal status and recovery in CD. However, further
609 studies should be conducted to evaluate the correlation between enterocyte protein expression,
610 treatment status and tissue histology.
611
612 The 4 analyzed TCD patients that developed morphological changes on day 4 after gluten
613 challenge displayed coordinated increase in expression of proteins that reflect rapid tissue
614 remodeling. This expression pattern was not observed in our first patient group where we

compared UCD with TCD mucosa. Thus, these proteins likely reflect processes that occur soon after gluten challenge. Intriguingly, TG2 expression increased clearly in two of four patients on day 4 after challenge. Further studies are required to determine whether similar changes in protein expression occur in TCD patients that develop less pronounced morphological changes in response to gluten challenge.

The use of FFPE tissue material has become increasingly popular in particular for characterization of neoplastic tissue and tumor biomarker discovery but also immune mediated diseases. Such studies are often challenging due to heterogeneity of the patient material and limited knowledge about the underlying pathology. CD represents in this respect a unique, immune-mediated disease: we have substantial knowledge on the pathological adaptive immune processes and we can also control exposure to the antigen (gluten) that drives the tissue inflammation. The use of label-free quantification of protein expression allows for streamlined and simple sample work-up, which reduces potential experimental biases and other technical challenges that often arises from traditional label-based quantitative mass spectrometry approaches. We here show as proof-of-concept that label-free quantification of proteins from FFPE tissue sections by use of mass spectrometry allows for accurate characterization of the celiac intestine. By use of archival biopsy material and careful design of patient groups, this methodology represents a potent tool to decipher specific questions and the missing details of disease pathogenesis.

ACKNOWLEDGEMENTS:

We thank Margit Brottveit for recruitment of patients, Melinda Ráki for assistance with patient selection, Magnus Ø. Arntzen for help with the initial steps of data analysis, Rasmus Iversen for providing the Ig sequence database, Maria Stensland for undertaking proteomics analysis and Linda T. Dorg and Ellen Hellesylt for helping out with histochemistry work.

REFERENCES

1. Maier T, Guell M, Serrano L: Correlation of mRNA and protein in complex biological samples. FEBS Lett 2009, 583:3966-73.

2. Plotkin JB: Transcriptional regulation is only half the story. Mol Syst Biol 2010, 6:406.

3. Matzke MM, Brown JN, Gritsenko MA, Metz TO, Pounds JG, Rodland KD, Shukla AK, Smith RD, Waters KM, McDermott JE, Webb-Robertson BJ: A comparative analysis of computational approaches to relative protein quantification using peptide peak intensities in label-free LC-MS proteomics experiments. Proteomics 2013, 13:493-503.

4. Wisniewski JR, Dus K, Mann M: Proteomic workflow for analysis of archival formalin-fixed and paraffin-embedded clinical samples to a depth of 10 000 proteins. Proteomics Clin Appl 2013, 7:225-33.

5. Steiner C, Ducret A, Tille JC, Thomas M, McKee TA, Rubbia-Brandt L, Scherl A, Lescuyer P, Cutler P: Applications of mass spectrometry for quantitative protein analysis in formalin-fixed paraffin-embedded tissues. Proteomics 2014, 14:441-51.

6. Gustafsson OJ, Arentz G, Hoffmann P: Proteomic developments in the analysis of formalin-fixed tissue. Biochim Biophys Acta 2015, 1854:559-80.

664 7. Sollid LM, Jabri B: Triggers and drivers of autoimmunity: lessons from coeliac
665 disease. Nat Rev Immunol 2013, 13:294-302.
666 8. Douglas AP, Crabbe PA, Hobbs JR: Immunochemical studies on the serum, intestinal
667 secretions and intestinal mucosa in patients with adult celiac disease and other forms of the
668 celiac syndrome. Gastroenterology 1970, 59:414-25.
669 9. Baklien K, Brandtzaeg P, Fausa O: Immunoglobulins in jejunal mucosa and serum
670 from patients with adult coeliac disease. Scand J Gastroenterol 1977, 12:149-59.
671 10. Scott H, Ek J, Baklien K, Brandtzaeg P: Immunoglobulin-producing cells in jejunal
672 mucosa of children with coeliac disease on a gluten-free diet and after gluten challenge. Scand
673 J Gastroenterol 1980, 15:81-8.
674 11. Di Niro R, Mesin L, Zheng NY, Stamnaes J, Morrissey M, Lee JH, Huang M, Iversen
675 R, du Pre MF, Qiao SW, Lundin KE, Wilson PC, Sollid LM: High abundance of plasma cells
676 secreting transglutaminase 2-specific IgA autoantibodies with limited somatic hypermutation
677 in celiac disease intestinal lesions. Nat Med 2012, 18:441-5.
678 12. Molberg O, McAdam SN, Korner R, Quarsten H, Kristiansen C, Madsen L, Fugger L,
679 Scott H, Noren O, Roepstorff P, Lundin KE, Sjostrom H, Sollid LM: Tissue transglutaminase
680 selectively modifies gliadin peptides that are recognized by gut-derived T cells in celiac
681 disease. Nat Med 1998, 4:713-7.
682 13. Dorum S, Arntzen MO, Qiao SW, Holm A, Koehler CJ, Thiede B, Sollid LM,
683 Fleckenstein B: The preferred substrates for transglutaminase 2 in a complex wheat gluten
684 digest are peptide fragments harboring celiac disease T-cell epitopes. PLoS ONE 2010,
685 5:e14056.
686 14. Lundin KE, Scott H, Hansen T, Paulsen G, Halstensen TS, Fausa O, Thorsby E, Sollid
687 LM: Gliadin-specific, HLA-DQ(α1*0501,β1*0201) restricted T cells isolated from the small
688 intestinal mucosa of celiac disease patients. J Exp Med 1993, 178:187-96.

689 15. Bodd M, Raki M, Tollefsen S, Fallang LE, Bergseng E, Lundin KE, Sollid LM: HLA-
690 DQ2-restricted gluten-reactive T cells produce IL-21 but not IL-17 or IL-22. Mucosal
691 Immunol 2010, 3:594-601.
692 16. Molberg O, Kett K, Scott H, Thorsby E, Sollid LM, Lundin KE: Gliadin specific,
693 HLA DQ2-restricted T cells are commonly found in small intestinal biopsies from coeliac
694 disease patients, but not from controls. Scand J Immunol 1997, 46:103-9.
695 17. Meresse B, Chen Z, Ciszewski C, Tretiakova M, Bhagat G, Krausz TN, Raulet DH,
696 Lanier LL, Groh V, Spies T, Ebert EC, Green PH, Jabri B: Coordinated induction by IL15 of
697 a TCR-independent NKG2D signaling pathway converts CTL into lymphokine-activated
698 killer cells in celiac disease. Immunity 2004, 21:357-66.
699 18. Oberhuber G: Histopathology of celiac disease. Biomed Pharmacother 2000, 54:368-
700 72.
701 19. Haere P, Hoie O, Schulz T, Schonhardt I, Raki M, Lundin KE: Long-term mucosal
702 recovery and healing in celiac disease is the rule - not the exception. Scand J Gastroenterol
703 2016, 51:1439-46.
704 20. Bragde H, Jansson U, Jarlsfelt I, Soderman J: Gene expression profiling of duodenal
705 biopsies discriminates celiac disease mucosa from normal mucosa. Pediatr Res 2011, 69:530-
706 7.
707 21. Diosdado B, van Bakel H, Strengman E, Franke L, van Oort E, Mulder CJ, Wijmenga
708 C, Wapenaar MC: Neutrophil recruitment and barrier impairment in celiac disease: a genomic
709 study. Clin Gastroenterol Hepatol 2007, 5:574-81.
710 22. Simula MP, Cannizzaro R, Canzonieri V, Pavan A, Maiero S, Toffoli G, De Re V:
711 PPAR signaling pathway and cancer-related proteins are involved in celiac disease-associated
712 tissue damage. Mol Med 2010, 16:199-209.

713 23. Brottveit M, Beitnes AC, Tollefsen S, Bratlie JE, Jahnsen FL, Johansen FE, Sollid
714 LM, Lundin KE: Mucosal cytokine response after short-term gluten challenge in celiac
715 disease and non-celiac gluten sensitivity. Am J Gastroenterol 2013, 108:842-50.
716 24. Cox J, Mann M: MaxQuant enables high peptide identification rates, individualized
717 p.p.b.-range mass accuracies and proteome-wide protein quantification. Nat Biotechnol 2008,
718 26:1367-72.
719 25. Cox J, Neuhauser N, Michalski A, Scheltema RA, Olsen JV, Mann M: Andromeda: a
720 peptide search engine integrated into the MaxQuant environment. J Proteome Res 2011,
721 10:1794-805.
722 26. Lefranc MP, Giudicelli V, Ginestoux C, Bodmer J, Muller W, Bontrop R, Lemaitre M,
723 Malik A, Barbie V, Chaume D: IMGT, the international ImMunoGeneTics database. Nucleic
724 Acids Res 1999, 27:209-12.
725 27. Iversen R, Snir O, Stensland M, Kroll JE, Steinsbo O, Korponay-Szabo IR, Lundin
726 KEA, de Souza GA, Sollid LM: Strong clonal relatedness between serum and gut IgA despite
727 different plasma cell origins. Cell Rep 2017, 20:2357-67.
728 28. Deeb SJ, D'Souza RC, Cox J, Schmidt-Supprian M, Mann M: Super-SILAC allows
729 classification of diffuse large B-cell lymphoma subtypes by their protein expression profiles.
730 Mol Cell Proteomics 2012, 11:77-89.
731 29. Shannon P, Markiel A, Ozier O, Baliga NS, Wang JT, Ramage D, Amin N,
732 Schwikowski B, Ideker T: Cytoscape: a software environment for integrated models of
733 biomolecular interaction networks. Genome Res 2003, 13:2498-504.
734 30. Bindea G, Mlecnik B, Hackl H, Charoentong P, Tosolini M, Kirilovsky A, Fridman
735 WH, Pages F, Trajanoski Z, Galon J: ClueGO: a Cytoscape plug-in to decipher functionally
736 grouped gene ontology and pathway annotation networks. Bioinformatics 2009, 25:1091-3.

737 31. Razick S, Magklaras G, Donaldson IM: iRefIndex: a consolidated protein interaction
738 database with provenance. BMC Bioinformatics 2008, 9:405.
739 32. Szklarczyk D, Franceschini A, Wyder S, Forslund K, Heller D, Huerta-Cepas J,
740 Simonovic M, Roth A, Santos A, Tsafou KP, Kuhn M, Bork P, Jensen LJ, von Mering C:
741 STRING v10: protein-protein interaction networks, integrated over the tree of life. Nucleic
742 Acids Res 2015, 43:D447-52.
743 33. Bankhead P, Loughrey MB, Fernandez JA, Dombrowski Y, McArt DG, Dunne PD,
744 McQuaid S, Gray RT, Murray LJ, Coleman HG, James JA, Salto-Tellez M, Hamilton PW:
745 QuPath: Open source software for digital pathology image analysis. Sci Rep 2017, 7:16878.
746 34. Schneider CA, Rasband WS, Eliceiri KW: NIH Image to ImageJ: 25 years of image
747 analysis. Nat Methods 2012, 9:671-5.
748 35. Schindelin J, Arganda-Carreras I, Frise E, Kaynig V, Longair M, Pietzsch T, Preibisch
749 S, Rueden C, Saalfeld S, Schmid B, Tinevez JY, White DJ, Hartenstein V, Eliceiri K,
750 Tomancak P, Cardona A: Fiji: an open-source platform for biological-image analysis. Nat
751 Methods 2012, 9:676-82.
752 36. Cox J, Hein MY, Luber CA, Paron I, Nagaraj N, Mann M: Accurate proteome-wide
753 label-free quantification by delayed normalization and maximal peptide ratio extraction,
754 termed MaxLFQ. Mol Cell Proteomics 2014, 13:2513-26.
755 37. Adriaanse MPM, Mubarak A, Riedl RG, Ten Kate FJW, Damoiseaux J, Buurman
756 WA, Houwen RHJ, Vreugdenhil ACE, Celiac Disease Study G: Progress towards non-
757 invasive diagnosis and follow-up of celiac disease in children; a prospective multicentre study
758 to the usefulness of plasma I-FABP. Sci Rep 2017, 7:8671.
759 38. Steinsbo O, Henry Dunand CJ, Huang M, Mesin L, Salgado-Ferrer M, Lundin KE,
760 Jahnsen J, Wilson PC, Sollid LM: Restricted VH/VL usage and limited mutations in gluten-
761 specific IgA of coeliac disease lesion plasma cells. Nat Commun 2014, 5:4041.

762 39. Snir O, Mesin L, Gidoni M, Lundin KE, Yaari G, Sollid LM: Analysis of celiac
763 disease autoreactive gut plasma cells and their corresponding memory compartment in
764 peripheral blood using high-throughput sequencing. J Immunol 2015, 194:5703-12.
765 40. Roy B, Neumann RS, Snir O, Iversen R, Sandve GK, Lundin KEA, Sollid LM: High-
766 throughput single-cell analysis of B cell receptor usage among autoantigen-specific plasma
767 cells in celiac cisease. J Immunol 2017, 199:782-91.
768 41. Bodd M, Raki M, Bergseng E, Jahnsen J, Lundin KE, Sollid LM: Direct cloning and
769 tetramer staining to measure the frequency of intestinal gluten-reactive T cells in celiac
770 disease. Eur J Immunol 2013, 43:2605-12.
771 42. Wilhelm M, Schlegl J, Hahne H, Gholami AM, Lieberenz M, Savitski MM, Ziegler E,
772 Butzmann L, Gessulat S, Marx H, Mathieson T, Lemeer S, Schnatbaum K, Reimer U,
773 Wenschuh H, Mollenhauer M, Slotta-Huspenina J, Boese JH, Bantscheff M, Gerstmair A,
774 Faerber F, Kuster B: Mass-spectrometry-based draft of the human proteome. Nature 2014,
775 509:582-7.
776 43. Platanias LC: Mechanisms of type-I- and type-II-interferon-mediated signalling. Nat
777 Rev Immunol 2005, 5:375-86.
778 44. Shiner M: Ultrastructural changes suggestive of immune reactions in the jejunal
779 mucosa of coeliac children following gluten challenge. Gut 1973, 14:1-12.
780 45. Shiner M, Ballard J: Antigen-antibody reactions in jejunal mucosa in childhood
781 coeliac disease after gluten challenge. Lancet 1972, 1:1202-5.
782 46. Lancaster-Smith M, Packer S, Kumar PJ, Harries JT: Immunological phenomena in
783 the jejunum and serum after reintroduction of dietary gluten in children with treated coeliac
784 disease. J Clin Pathol 1976, 29:592-7.

785 47. Sarna VK, Skodje GI, Reims HM, Risnes LF, Dahal-Koirala S, Sollid LM, Lundin
786 KEA: HLA-DQ:gluten tetramer test in blood gives better detection of coeliac patients than
787 biopsy after 14-day gluten challenge. Gut 2017.
788 48. Raki M, Fallang LE, Brottveit M, Bergseng E, Quarsten H, Lundin KE, Sollid LM:
789 Tetramer visualization of gut-homing gluten-specific T cells in the peripheral blood of celiac
790 disease patients. Proc Natl Acad Sci U S A 2007, 104:2831-6.
791 49. Brottveit M, Raki M, Bergseng E, Fallang LE, Simonsen B, Lovik A, Larsen S,
792 Loberg EM, Jahnsen FL, Sollid LM, Lundin KE: Assessing possible celiac disease by an
793 HLA-DQ2-gliadin Tetramer Test. Am J Gastroenterol 2011, 106:1318-24.
794 50. Han A, Newell EW, Glanville J, Fernandez-Becker N, Khosla C, Chien YH, Davis
795 MM: Dietary gluten triggers concomitant activation of CD4+ and CD8+ αβ T cells and γδ T
796 cells in celiac disease. Proc Natl Acad Sci U S A 2013, 110:13073-8.
797 51. Beitnes AC, Raki M, Brottveit M, Lundin KE, Jahnsen FL, Sollid LM: Rapid
798 accumulation of CD14+CD11c+ dendritic cells in gut mucosa of celiac disease after in vivo
799 gluten challenge. PLoS ONE 2012, 7:e33556.
800 52. Beitnes AC, Raki M, Lundin KE, Jahnsen J, Sollid LM, Jahnsen FL: Density of
801 CD163+ CD11c+ dendritic cells increases and CD103+ dendritic cells decreases in the
802 coeliac lesion. Scand J Immunol 2011, 74:186-94.
803 53. Hallgren R, Colombel JF, Dahl R, Fredens K, Kruse A, Jacobsen NO, Venge P,
804 Rambaud JC: Neutrophil and eosinophil involvement of the small bowel in patients with
805 celiac disease and Crohn's disease: studies on the secretion rate and immunohistochemical
806 localization of granulocyte granule constituents. The American journal of medicine 1989,
807 86:56-64.
808 54. Moran CJ, Kolman OK, Russell GJ, Brown IS, Mino-Kenudson M: Neutrophilic
809 infiltration in gluten-sensitive enteropathy is neither uncommon nor insignificant: assessment

of duodenal biopsies from 267 pediatric and adult patients. Am J Surg Pathol 2012, 36:1339-45.

55. Nilsen EM, Lundin KE, Krajci P, Scott H, Sollid LM, Brandtzaeg P: Gluten specific, HLA-DQ restricted T cells from coeliac mucosa produce cytokines with Th1 or Th0 profile dominated by interferon gamma. Gut 1995, 37:766-76.

56. Monteleone G, Pender SL, Alstead E, Hauer AC, Lionetti P, McKenzie C, MacDonald TT: Role of interferon alpha in promoting T helper cell type 1 responses in the small intestine in coeliac disease. Gut 2001, 48:425-9.

57. Raki M, Beitnes AC, Lundin KE, Jahnsen J, Jahnsen FL, Sollid LM: Plasmacytoid dendritic cells are scarcely represented in the human gut mucosa and are not recruited to the celiac lesion. Mucosal Immunol 2013, 6:985-92.

58. Lilja JJ, Kivisto KT, Neuvonen PJ: Grapefruit juice-simvastatin interaction: effect on serum concentrations of simvastatin, simvastatin acid, and HMG-CoA reductase inhibitors. Clin Pharmacol Ther 1998, 64:477-83.

59. Moron B, Verma AK, Das P, Taavela J, Dafik L, Diraimondo TR, Albertelli MA, Kraemer T, Maki M, Khosla C, Rogler G, Makharia GK: CYP3A4-catalyzed simvastatin metabolism as a non-invasive marker of small intestinal health in celiac disease. Am J Gastroenterol 2013, 108:1344-51.

60. Derikx JP, Vreugdenhil AC, Van den Neucker AM, Grootjans J, van Bijnen AA, Damoiseaux JG, van Heurn LW, Heineman E, Buurman WA: A pilot study on the noninvasive evaluation of intestinal damage in celiac disease using I-FABP and L-FABP. J Clin Gastroenterol 2009, 43:727-33.

61. Adriaanse MP, Tack GJ, Passos VL, Damoiseaux JG, Schreurs MW, van Wijck K, Riedl RG, Masclee AA, Buurman WA, Mulder CJ, Vreugdenhil AC: Serum I-FABP as

marker for enterocyte damage in coeliac disease and its relation to villous atrophy and circulating autoantibodies. Aliment Pharmacol Ther 2013, 37:482-90.

62. Adriaanse MP, Leffler DA, Kelly CP, Schuppan D, Najarian RM, Goldsmith JD, Buurman WA, Vreugdenhil AC: Serum I-FABP Detects Gluten Responsiveness in Adult Celiac Disease Patients on a Short-Term Gluten Challenge. Am J Gastroenterol 2016, 111:1014-22.

TABLES

Table 1 Characteristics of CD patient before and after treatment

Patient	Age/sex	Marsh score		Serology (anti TG2 IgA)		IEL (per 100 EC)	
		UCD	TCD	UCD	TCD	UCD	TCD
P1	45/M	3B	1	3.3	<1	46.3	27.0
P2	22/F	3C	0	16.6	1.5	26.7	21.7
P3	23/F	3C	0	3.8	<1	36.3	15.7
P4	56/F	3C	1	4.8	<1	48.0	33.0
P5	54/F	3B	1	11	1.2	65.0	31.3
P6	44/M	3B	1	2.2	1.1	53.7	25.7
P7	58/M	3B	0	3.1	<1	38.3	15.7
P8	28/F	3B	1	23	<1	53.0	31.0
P9	38/F	3B	3A	7.8	1.6	45.0	28.0
P10	61/M	3C	3B	31.3	<1	18.7	28.3

Table 2 Characteristics of CD patients subject to 3 day gluten challenge

Patient	Age/ sex	Marsh score d0 before gluten challenge	Marsh score d4 after 3 day gluten challenge
B	47/F	1	3A
C	31/F	3A	3B
D	59/F	2	3A
E	53/F	0	3B

FIGURE LEGENDS

Figure 1. Differential protein expression in UCD versus TCD mucosa. A) Principal component analysis (PCA) of log2 transformed LFQ intensities of all identified proteins. UCD samples are shown as open circles and TCD samples as black filled circles. Technical replicates group together. B) Scatter plot of all proteins loaded for principal component analysis, where selected proteins that contribute strongly to separation of TCD and UCD are highlighted in red. C) Differentially expressed proteins in UCD (M3) compared to TCD (M0-1) mucosa visualized as volcano plot (two-sample t-test, FDR<0.01). The line defining the outliers is limited by the p-value in the y axis and the S0 value (0.5) in the x-axis. Selected proteins with strong differential expression are indicated in red. D) Hierarchical clustering of log2 transformed LFQ intensities of differentially expressed proteins separates UCD and TCD. (Yellow = 32, Blue = 18).

Figure 2. Proteins involved in nutrient metabolism and enterocyte function show reduced expression in UCD mucosa and increased expression in TCD mucosa. A) GO biological process enrichment analysis of proteins significantly upregulated in TCD mucosa. Each pathway is shown as a node and node size reflects enrichment p-value. Groups are formed based on the number of shared proteins between the pathways (>50%). For most groups the GO term with the lowest p-value is shown in bold. Nodes with split colors indicate processes that fit to several groups. Edges indicate that proteins are shared between the processes (nodes). B) Comparison of log2 transformed LFQ intensities for selected proteins before (UCD) or after (TCD) GFD for all patients except P9.

Figure 3. Increased expression of plasma cell related processes and immunoglobulins in UCD mucosa. A) GO biological process enrichment analysis of proteins significantly

875 increased UCD (M3) mucosa. Of 143 annotated genes, 88 are represented in enriched
876 biological processes. These can broadly be divided into immune response processes, and
877 protein synthesis and ER stress. B) Principal component analysis of log2 transformed LFQ
878 intensities of identified Ig family members from MaxQuant search against dedicated Ig
879 database. UCD samples are shown as open circles and TCD samples as black filled circles.
880 Median of technical replicates are used. C) Scatter plot of all proteins loaded for principal
881 component analysis. Proteins identified from one, or more than one peptide, are shown as
882 open or filled circles respectively. The gene name of the leading razor protein is shown. D)
883 Differential expression of Igs in UCD (M3) compared to TCD (M0-1) mucosa visualized as
884 volcano plot (two-sample t-test, FDR<0.05, S0= 0.5). Proteins identified by one or more than
885 one peptide are shown as open or filled (grey and red) circles respectively. Selected proteins
886 are shown in red. Allotypes are indicated for IGHV3-15*02 and *08 as both were identified
887 from two unique peptides of comparable quality (data not shown). E) Comparison of log2
888 transformed LFQ intensities for selected Igs before (UCD) or after GFD (TCD). Patient P7 is
889 shown in red.
890
891 **Figure 4 Increase of neutrophils and monocyte-derived cells in UCD mucosa is reflected**
892 **in the proteome expression profile.**
893 A) Twenty-six of the significantly increased proteins in UCD mucosa map to the GO
894 Reactome pathway "Neutrophil degranulation". B) Density of CD15, MPO and calprotectin
895 positive cells in the duodenal lamina propria of 5 patients comparing UCD and TCD samples.
896 Data points represent mean counts for individual patients and box plots denotes minimum,
897 maximum and median values in the group. C) LFQ intensity values for MPO and calprotectin
898 (S1008A and S1009A) for the same patients as shown in B). Datapoints represent values from
899 individual patients and box plot denotes minimum, maximum and median values in the group.

D) Representative images showing immunofluorescence co-staining for CD15, CD163 and calprotectin or MPO. Merged images were pseudo-colored in Image J and single channel images are shown in grayscale. Arrowheads denote single or double positive cells, representing neutrophils (green) and monocyte derived cells (white).

Figure 5. Protein-protein interaction analysis reveals dominant cytokine responses. A) Protein interaction network filtered on response to cytokine as described in Materials and Methods. All identified proteins were considered for PPI analysis and filtered based on "response to cytokine". T-test significant proteins are shown as large nodes and node border indicate higher expression in UCD (red) or in TCD (green). Nodes were further colored according to presence in three selected GO terms, other proteins are colored grey. B) Comparison of log2 transformed LFQ intensities for selected proteins central to the cytokine responses.

Figure 6. Differential protein expression in TCD patients before and after 3-day gluten challenge A) Differentially expressed proteins in mucosa of TCD patients before (d0) or after 3-day gluten challenge (d4) visualized by volcano plot (two-sample t-test, FDR<0.05, S0 = 0.5). Selected proteins are shown in red. B) Hierarchical clustering of log2 transformed LFQ intensities of differentially expressed proteins will group samples as before or after gluten challenge. (Yellow = 32, Blue = 18).

Figure 7. Proteins involved in tissue remodeling are upregulated in response to gluten challenge. A) GO biological process enrichment analysis of proteins significantly upregulated following 3-day gluten challenge. B) STRING protein-protein interaction analysis of significantly upregulated proteins resulted in 135 protein-protein interaction (edges). Selected

proteins are manually color coded to show occurrence in enriched GO biological process as shown in A) in addition to the GO term “Wound healing”. Transglutaminase 2 (TGM2) is indicated in yellow. C) Comparison of log2 transformed LFQ intensities for selected proteins involved in tissue remodeling and the autoantigen TGM2 for patients before and after 3-day challenge, and patients P1-P8 and P10 UCD versus TCD.

SI Figure 1 Verification of LFQ normalization

Comparison of LFQ intensities of spiked proteins and peptides for samples P1-P10 where s18 is P9 after GFD (TCD).

SI Figure 2 Comparison of LFQ normalization from human (UniProt) or Ig database searches

Comparison of log2 transformed LFQ intensities of Ig constant region identifications that are shared between the databases (A) and spiked proteins (B).

SI Figure 3 Neutrophil infiltration in UCD compared to TCD

Selected regions from two patients showing CD15 staining used for neutrophil density assessment in Figure 4B. CD15 is a carbohydrate that also can be expressed by enterocytes and goblet cells, giving rise to epithelial cell staining.

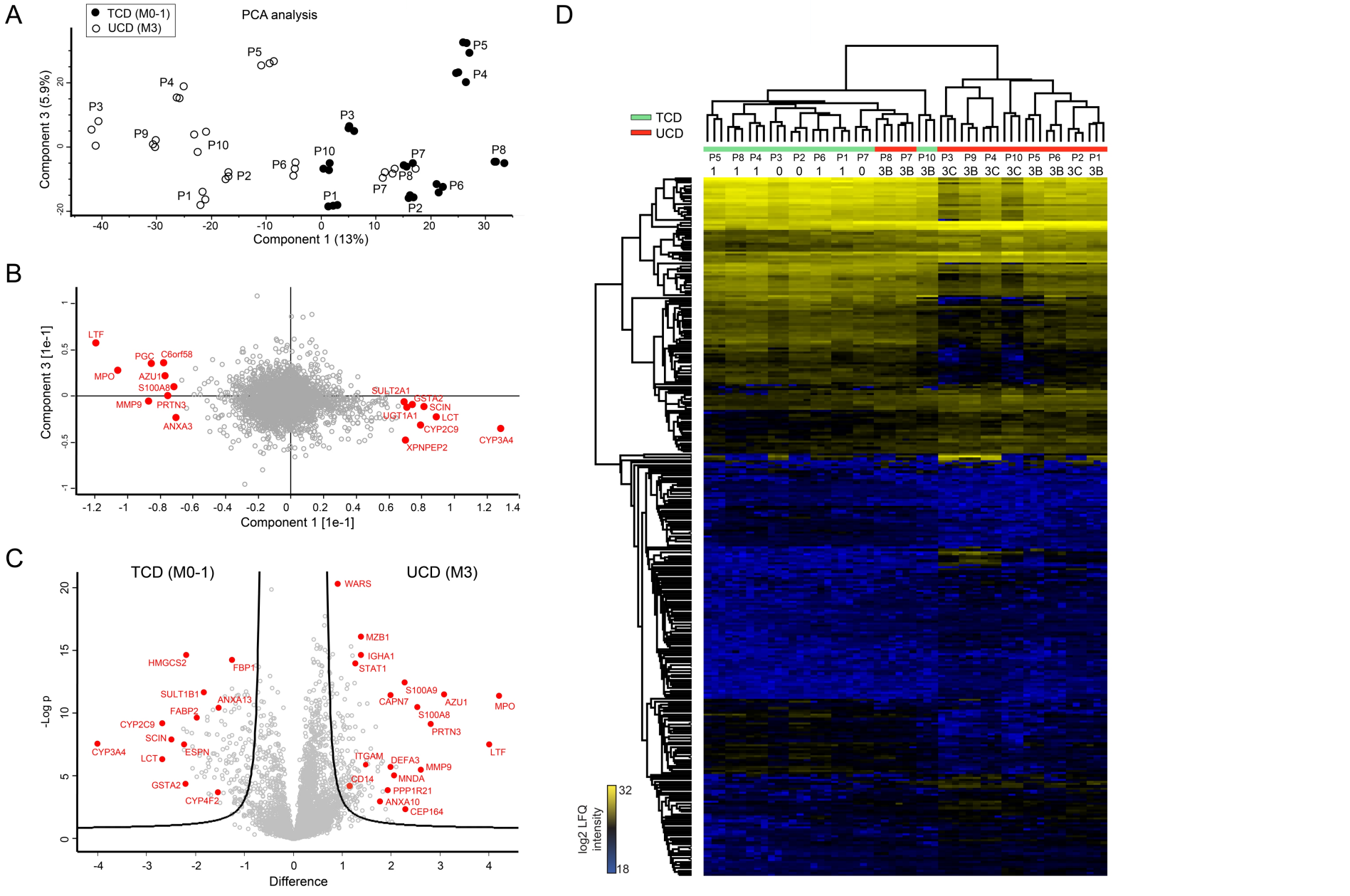
A
TCD (M0-1)
UCD (M3)
PCA analysis
Component 3 (5.9%)
Component 1 (13%)
B
Component 3 [1e-1]
Component 1 [1e-1]
LTF
PGC
C6orf58
MPO
AZU1
S100A8
MMP9
PRTN3
ANXA3
SULT2A1
GSTA2
SCIN
UGT1A1
LCT
CYP2C9
XPNPEP2
CYP3A4
C
TCD (M0-1)
UCD (M3)
-Log p
Difference
WARS
MZB1
IGHA1
STAT1
HMGCS2
FBP1
SULT1B1
ANXA13
FABP2
CYP2C9
SCIN
CYP3A4
LCT
ESPN
GSTA2
CYP4F2
S100A9
CAPN7
AZU1
MPO
S100A8
PRTN3
LTF
ITGAM
DEFA3
MMP9
CD14
MNDA
PPP1R21
ANXA10
CEP164
D
TCD
UCD
P5 P8 P4 P3 P2 P6 P1 P7 P8 P7 P10 P3 P9 P4 P10 P5 P6 P2 P1
1 1 1 0 0 1 1 0 3B 3B 3B 3C 3B 3C 3C 3B 3B 3C 3B
log2 LFQ intensity
32
18

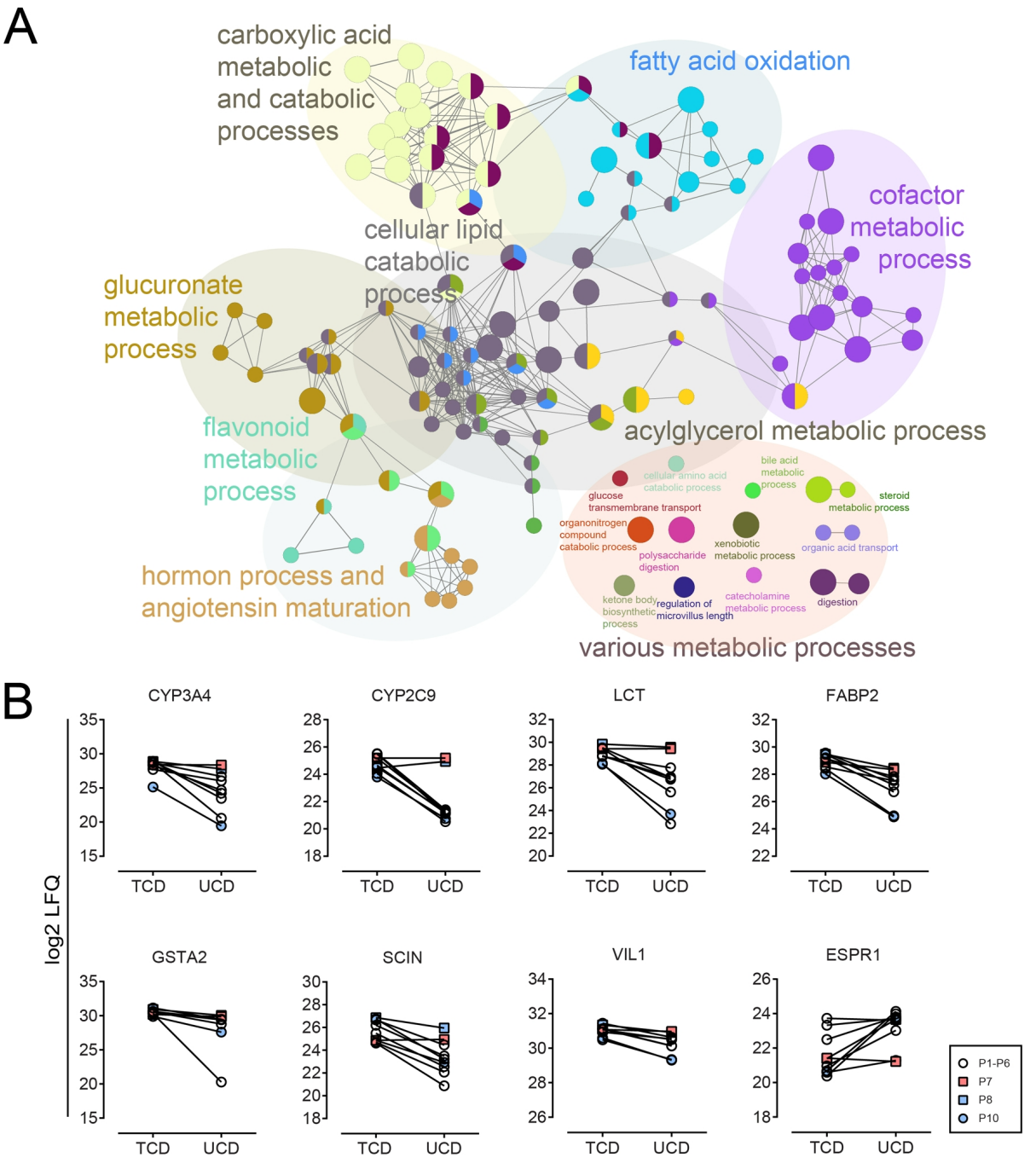
A
carboxylic acid metabolic and catabolic processes
fatty acid oxidation
cofactor metabolic process
cellular lipid catabolic process
glucuronate metabolic process
flavonoid metabolic process
acylglycerol metabolic process
hormon process and angiotensin maturation
various metabolic processes
cellular amino acid catabolic process
bile acid metabolic process
glucose transmembrane transport
steroid metabolic process
organonitrogen compound catabolic process
xenobiotic metabolic process
organic acid transport
polysaccharide digestion
ketone body biosynthetic process
regulation of microvillus length
catecholamine metabolic process
digestion
B
log2 LFQ
CYP3A4
CYP2C9
LCT
FABP2
GSTA2
SCIN
VIL1
ESPR1
TCD
UCD
P1-P6
P7
P8
P10

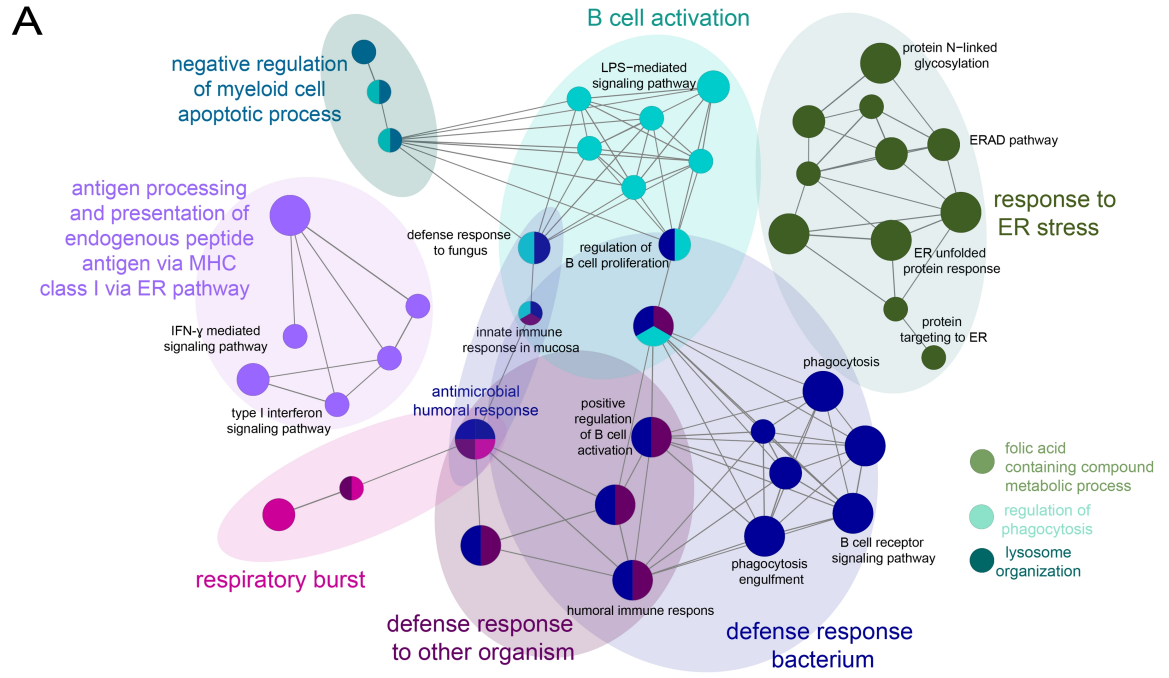

Immunoglobulin gene family identifications

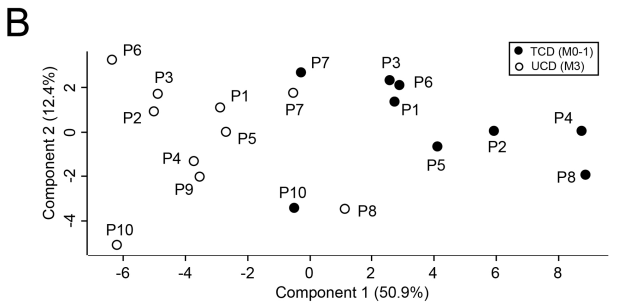

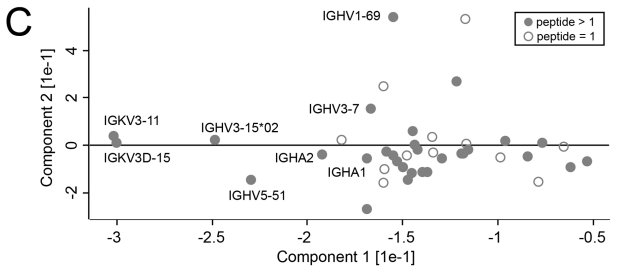

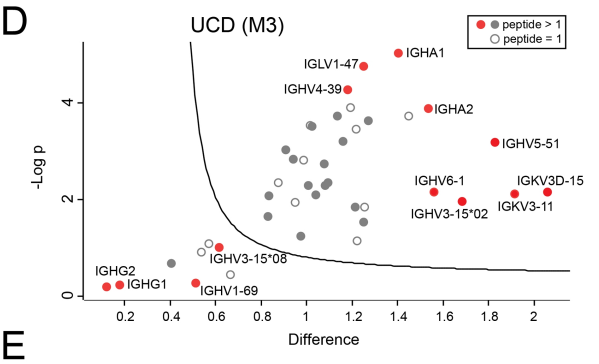

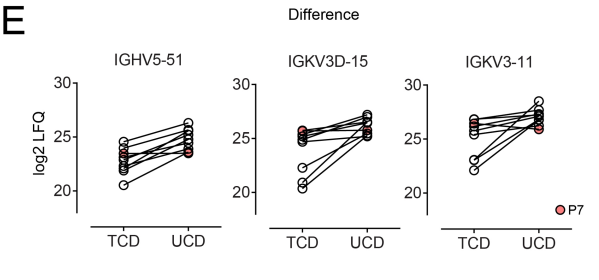

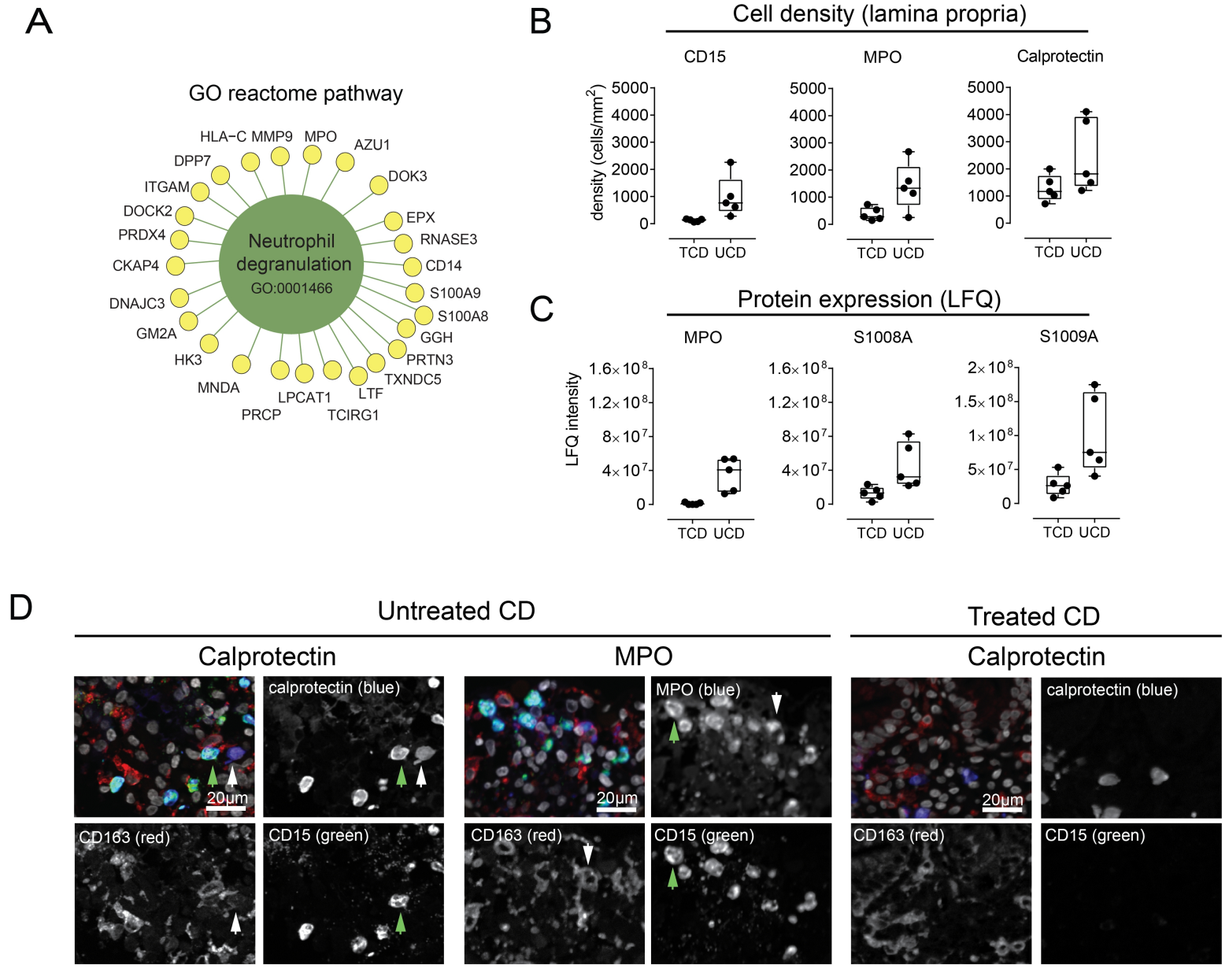
A
GO reactome pathway
Neutrophil degranulation
GO:0001466
HLA−C
MMP9
MPO
AZU1
DOK3
EPX
RNASE3
CD14
S100A9
S100A8
GGH
PRTN3
TXNDC5
LTF
TCIRG1
LPCAT1
PRCP
MNDA
HK3
GM2A
DNAJC3
CKAP4
PRDX4
DOCK2
ITGAM
DPP7
B
Cell density (lamina propria)
CD15
MPO
Calprotectin
density (cells/mm2)
5000
4000
3000
2000
1000
0
TCD UCD
C
Protein expression (LFQ)
MPO
S1008A
S1009A
LFQ intensity
1.6×10^8
1.2×10^8
8×10^7
4×10^7
0
2×10^8
1.5×10^8
1×10^8
5×10^7
TCD UCD
D
Untreated CD
Treated CD
Calprotectin
MPO
Calprotectin
calprotectin (blue)
MPO (blue)
20μm
CD163 (red)
CD15 (green)

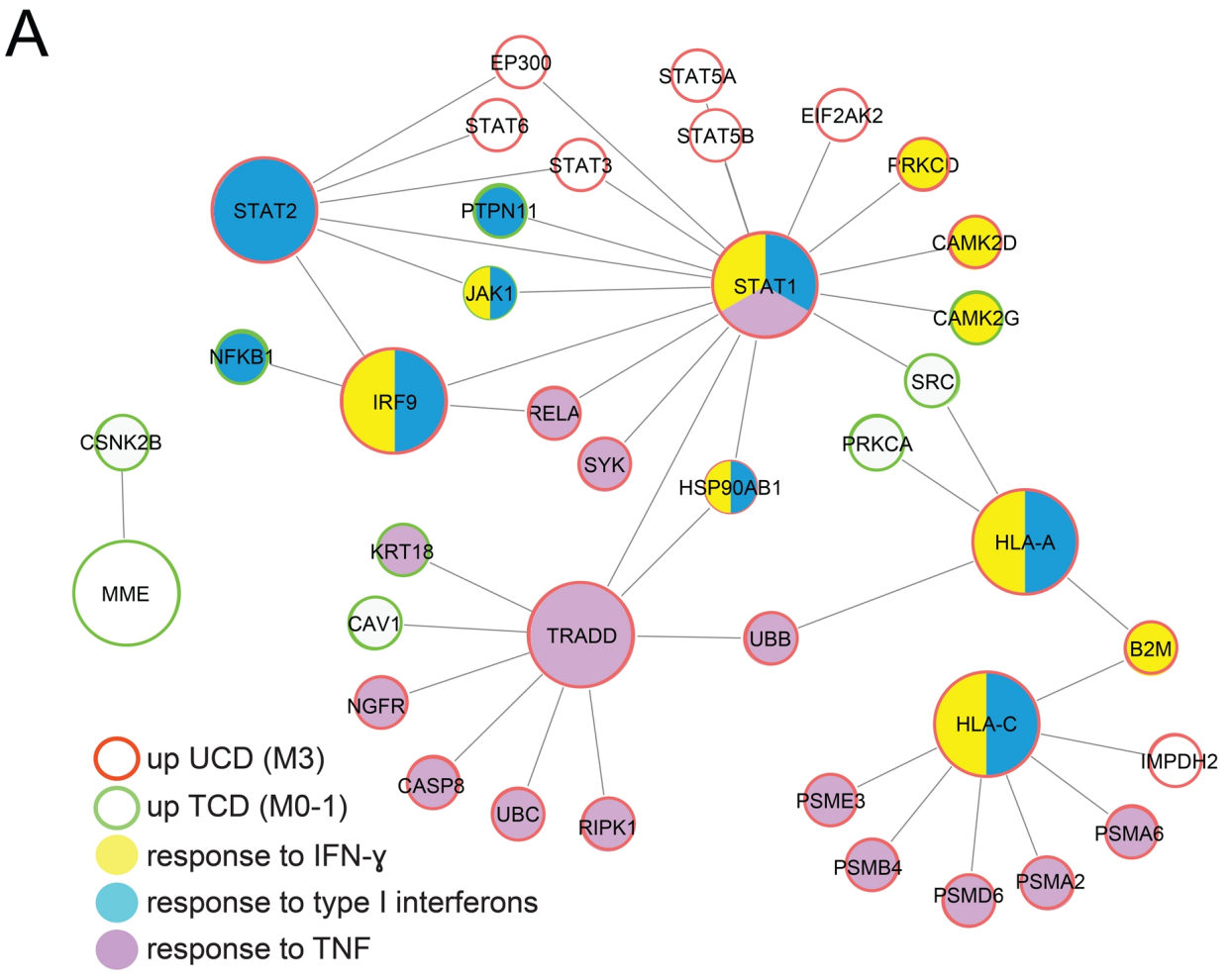
A
EP300
STAT5A
STAT6
STAT5B
EIF2AK2
STAT3
PRKCD
STAT2
PTPN11
CAMK2D
STAT1
JAK1
CAMK2G
NFKB1
SRC
IRF9
RELA
CSNK2B
PRKCA
SYK
HSP90AB1
HLA-A
KRT18
MME
CAV1
TRADD
UBB
B2M
NGFR
HLA-C
IMPDH2
CASP8
PSME3
UBC
RIPK1
PSMA6
PSMB4
PSMD6
PSMA2
up UCD (M3)
up TCD (M0-1)
response to IFN-γ
response to type I interferons
response to TNF

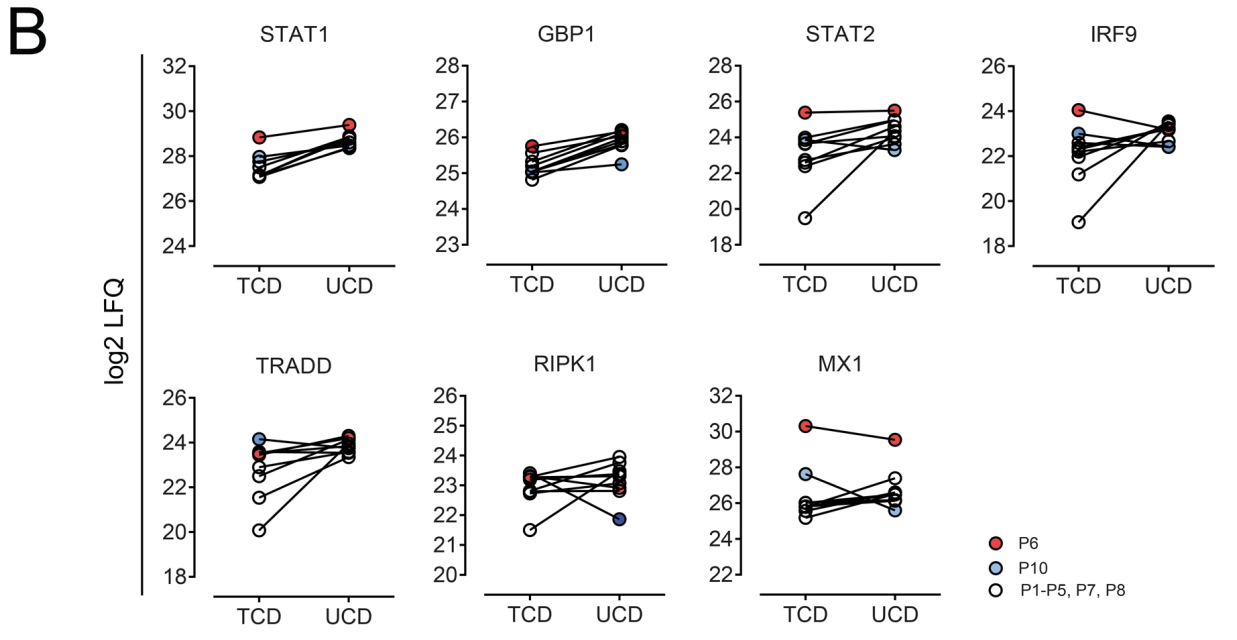
B
STAT1
GBP1
STAT2
IRF9
TRADD
RIPK1
MX1
log2 LFQ
TCD
UCD
P6
P10
P1-P5, P7, P8

A

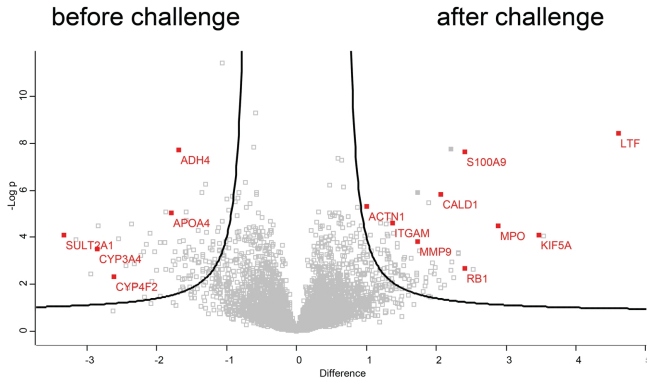
before challenge
after challenge
-Log p
Difference
ADH4
APOA4
SULT2A1
CYP3A4
CYP4F2
ACTN1
ITGAM
MMP9
RB1
CALD1
S100A9
LTF
MPO
KIF5A

B

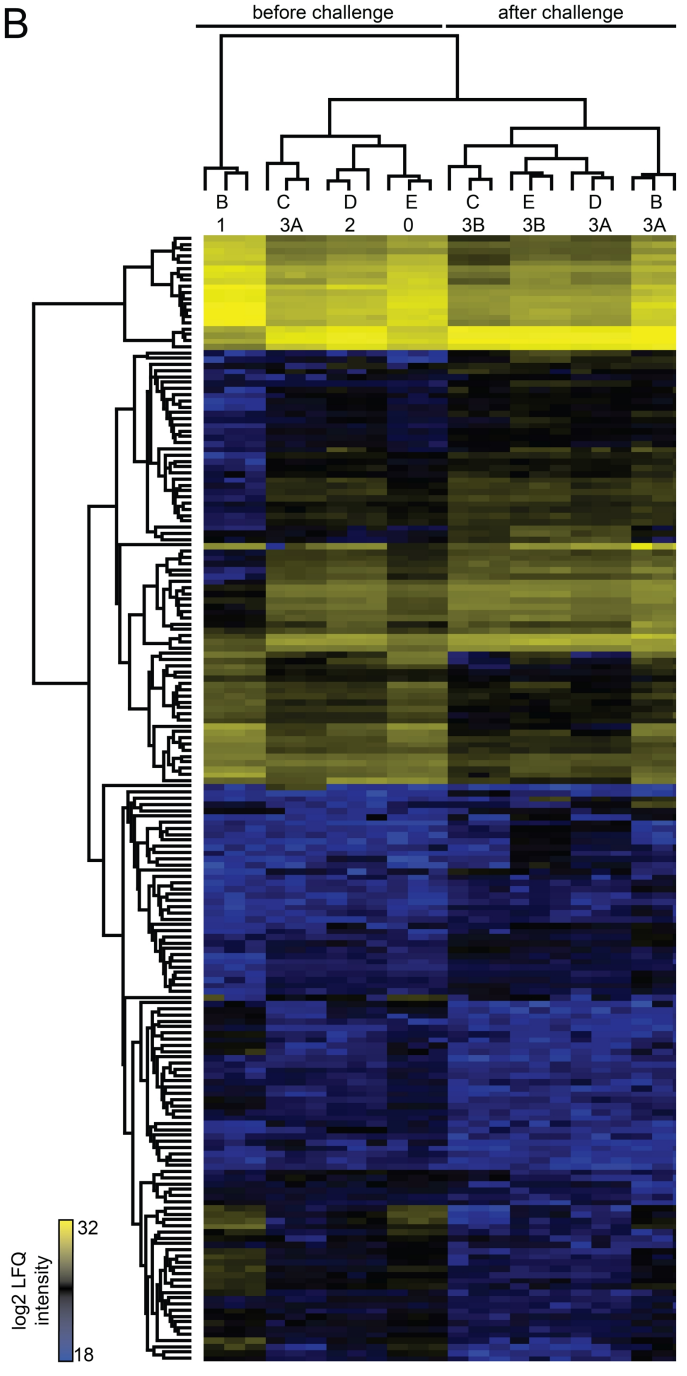
before challenge
after challenge
B 1
C 3A
D 2
E 0
C 3B
E 3B
D 3A
B 3A
log2 LFQ intensity
32
18

A

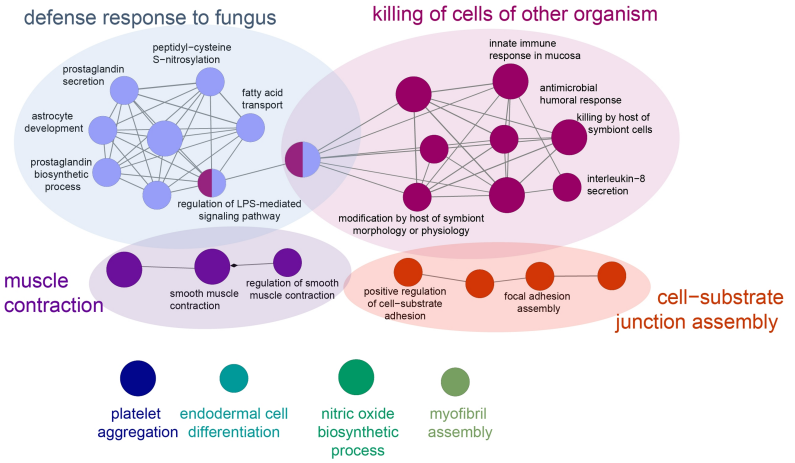
defense response to fungus
killing of cells of other organism
peptidyl−cysteine S−nitrosylation
prostaglandin secretion
fatty acid transport
astrocyte development
prostaglandin biosynthetic process
regulation of LPS−mediated signaling pathway
innate immune response in mucosa
antimicrobial humoral response
killing by host of symbiont cells
interleukin−8 secretion
modification by host of symbiont morphology or physiology
muscle contraction
smooth muscle contraction
regulation of smooth muscle contraction
positive regulation of cell−substrate adhesion
focal adhesion assembly
cell−substrate junction assembly
platelet aggregation
endodermal cell differentiation
nitric oxide biosynthetic process
myofibril assembly

B

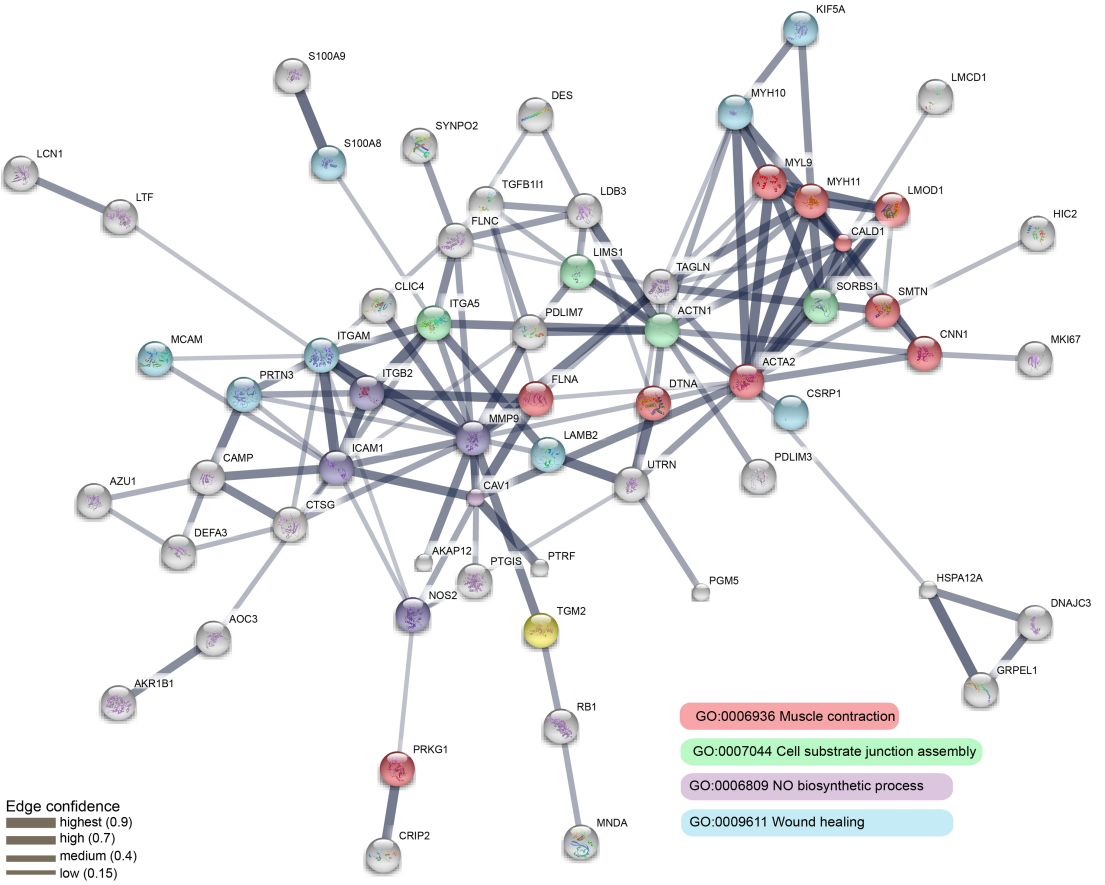
KIF5A
S100A9
LMCD1
MYH10
DES
SYNPO2
S100A8
LCN1
MYL9
MYH11
LMOD1
LTF
TGFB1I1
LDB3
HIC2
FLNC
CALD1
LIMS1
TAGLN
CLIC4
SORBS1
SMTN
ITGA5
PDLIM7
ACTN1
MCAM
ITGAM
CNN1
MKI67
ACTA2
PRTN3
ITGB2
FLNA
DTNA
CSRP1
MMP9
LAMB2
CAMP
ICAM1
PDLIM3
AZU1
CAV1
UTRN
CTSG
DEFA3
AKAP12
PTGIS
PTRF
PGM5
HSPA12A
DNAJC3
NOS2
TGM2
AOC3
GRPEL1
AKR1B1
RB1
PRKG1
MNDA
CRIP2
GO:0006936 Muscle contraction
GO:0007044 Cell substrate junction assembly
GO:0006809 NO biosynthetic process
GO:0009611 Wound healing
Edge confidence
highest (0.9)
high (0.7)
medium (0.4)
low (0.15)

C

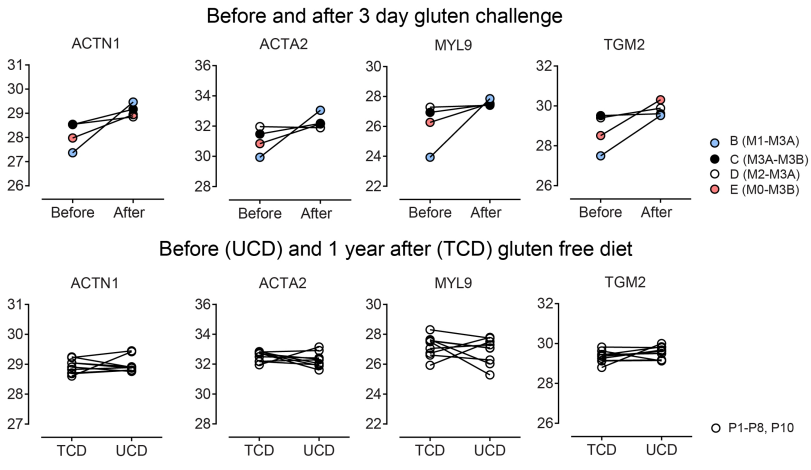
Before and after 3 day gluten challenge
ACTN1
ACTA2
MYL9
TGM2
Before
After
B (M1-M3A)
C (M3A-M3B)
D (M2-M3A)
E (M0-M3B)
Before (UCD) and 1 year after (TCD) gluten free diet
TCD
UCD
P1-P8, P10

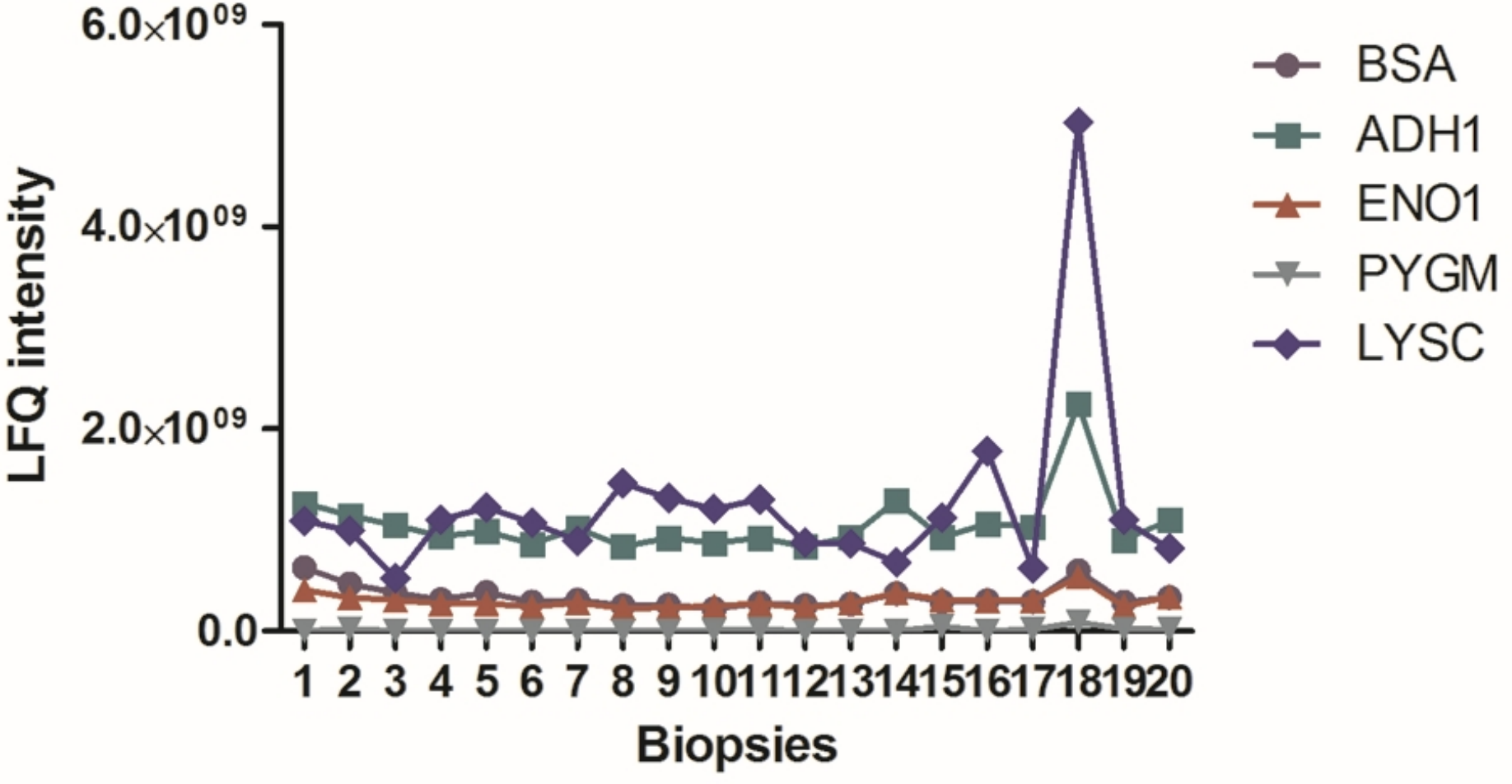
6.0×10^09
4.0×10^09
2.0×10^09
0.0
LFQ intensity
1 2 3 4 5 6 7 8 9 10 11 12 13 14 15 16 17 18 19 20
Biopsies
BSA
ADH1
ENO1
PYGM
LYSC

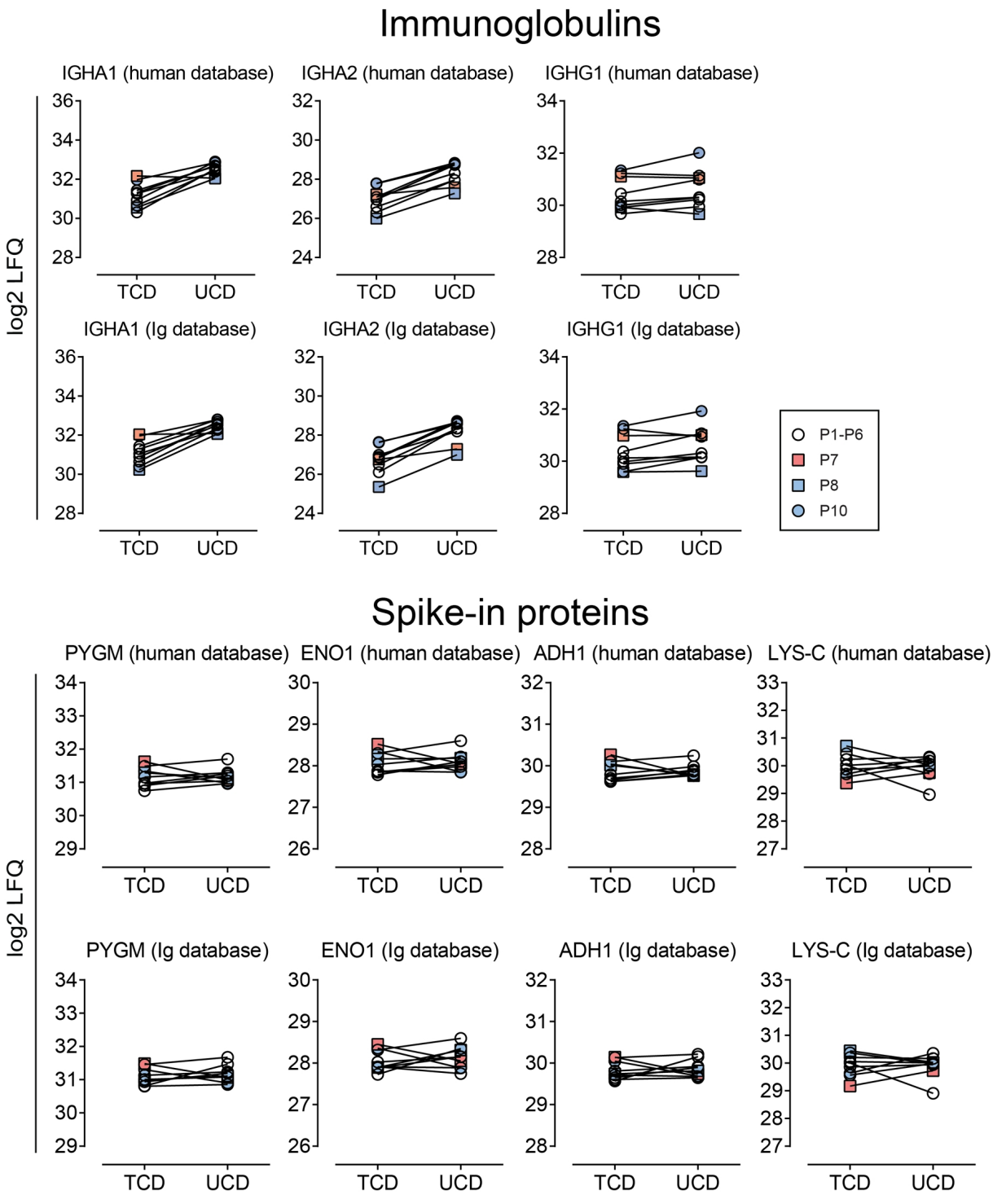
Immunoglobulins
IGHA1 (human database)
IGHA2 (human database)
IGHG1 (human database)
IGHA1 (Ig database)
IGHA2 (Ig database)
IGHG1 (Ig database)
log2 LFQ
TCD
UCD
P1-P6
P7
P8
P10
Spike-in proteins
PYGM (human database)
ENO1 (human database)
ADH1 (human database)
LYS-C (human database)
PYGM (Ig database)
ENO1 (Ig database)
ADH1 (Ig database)
LYS-C (Ig database)

CD15 staining

UCD

TCD

P1

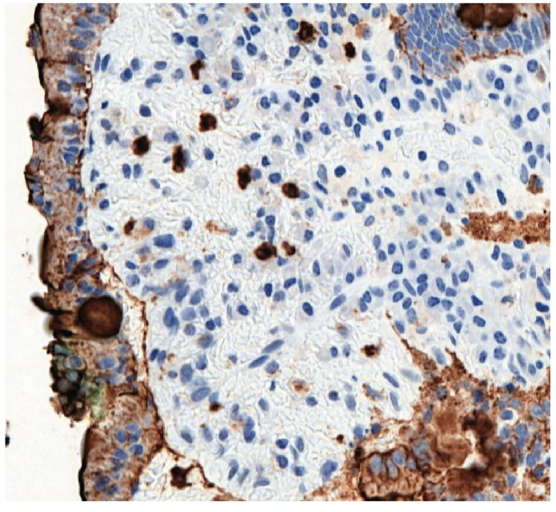

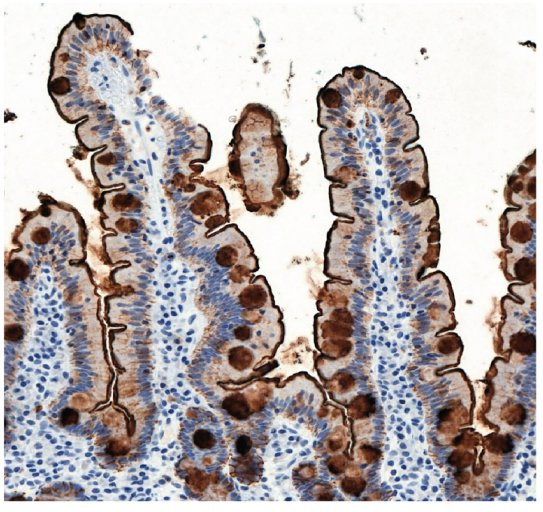
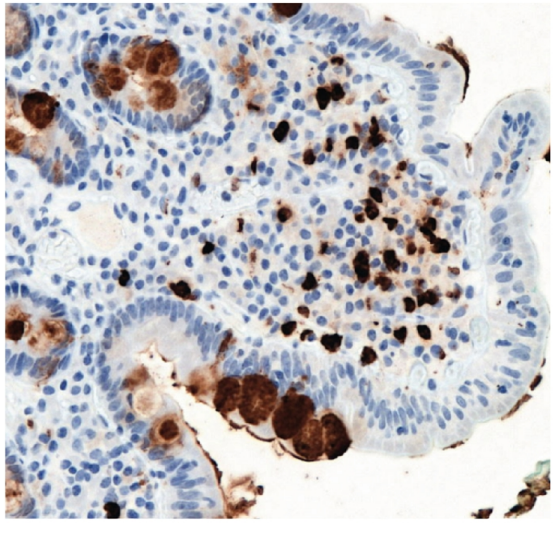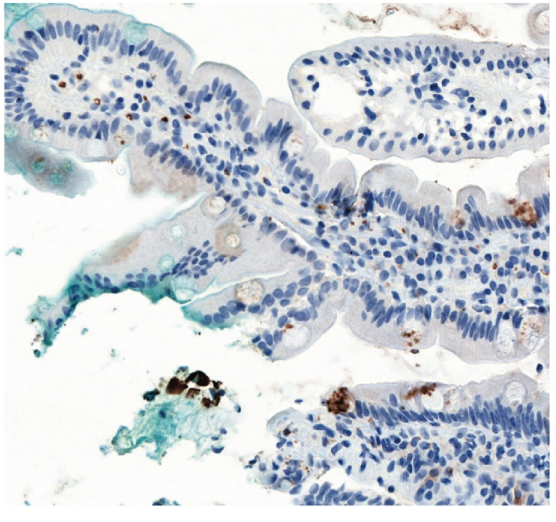
P6